

The role of short-term synaptic plasticity in neuronal microcircuit

Jin Bao

born in Hefei, China

Biology Faculty

Georg-August-University Göttingen

A thesis submitted for the degree of

Philosophiæ Doctor (PhD)

2010

Göttingen

1. Reviewer: Prof. Dr. Erwin Neher

2. Reviewer: Prof. Dr. Ralf Heinrich

Day of the defense: 08.07.2010

Abstract

Neuronal microcircuit is built by neurons connected with dynamic synapses. Short-term synaptic plasticity is one form of the synaptic dynamics, which plays various roles in the circuit information processing and computation. To analyze the function of short-term synaptic plasticity in feed-forward inhibitory (FFI) circuits, electrophysiological experiments on acute mice brain slices and computational model simulations have been applied. Feed-forward inhibitory circuit is composed of an excitatory input synapse, an interneuron and an inhibitory output synapse. Two cerebellar FFI circuits (basket cell mediating somatic FFI and stellate cell mediating dendritic FFI) have been analyzed in parallel in this work to compare their input/output synaptic dynamics, the intrinsic firing property of interneurons and the circuit output dynamics. It is shown that these two FFI circuits differ only on their input synaptic dynamics, and their circuit output dynamics are tightly regulated by the input synaptic dynamics because the interneurons (both basket and stellate cell) transform the magnitude of the synaptic input into the rate of their firing output lineally. Computational simulation has further demonstrated that the circuit output dynamics is determined to be depressing when the input synapse is depressing, while the output is a balance between the input and output synaptic dynamics when the input synapse shows facilitation. In summary, short-term synaptic plasticity performs the temporal tuning function in the neuronal circuit.

Contents

List of Figures	iii
List of Tables	v
1 Introduction	1
1.1 Part one: synaptic transmission	1
1.2 Part two: Short-term synaptic plasticity (STP)	6
1.3 Part three: The Computational function of STP	13
2 Materials & Methods	19
2.1 Cellular organization of cerebellar cortex	19
2.2 Acute brain slice preparation	21
2.3 Slice patch clamp recording	22
2.3.1 Patch clamp recording setup	22
2.3.2 How to identify a healthy neuron in the slice	24
2.3.3 Whole-cell patch clamp of a neuron in the slice	24
2.3.4 Dendritic patch clamp recording	26
2.3.5 Simultaneous multi-neuron recording	27
2.4 Extracellular stimulation	27
2.5 Dynamic clamp	28
2.6 Data analysis and computer simulations	30
2.6.1 Experimental data analysis	30
2.6.2 Simulating the model circuit	30

CONTENTS

3	Results	35
3.1	Cerebellar feed-forward inhibitory (FFI) circuits	35
3.2	Various forms of STP in the FFI circuit	39
3.2.1	Target-dependent STP of excitatory synapses	39
3.2.2	Depressing inhibitory synapses	41
3.3	Interactions of STP in the FFI circuit	42
3.3.1	Predicting circuit dynamics from a model circuit	43
3.3.2	Spike output dynamics of interneurons are regulated by input synaptic dynamics	46
3.3.3	Facilitating synapses connected to depressing synapses	47
3.3.4	Two depressing synapses in series	51
3.4	Change of synaptic dynamics alters circuit dynamics	54
3.4.1	Munc13-3 knockout mice turns depressing synapses to facilitating synapses	54
3.4.2	Simulating artificial synaptic dynamics with dynamic clamp	56
4	Discussion	59
4.1	The determinants of neuronal circuit dynamics	60
4.2	Mechanisms of target-dependent synaptic plasticity	61
4.3	Functional implications in cerebellar information processing	67
	References	71

List of Figures

1.1	A cartoon of a chemical synapse	2
1.2	The different forms of short-term synaptic plasticity	8
2.1	Three-layer organization of the cerebellar cortex	20
2.2	The mouse brain parasagittal view	22
2.3	The hardware design of the dynamic clamp	28
2.4	Leaky integrate-and-fire model	33
3.1	A cartoon of feed-forward inhibitory circuit	36
3.2	Cerebellar feed-forward inhibitory circuits	36
3.3	BC and SC share the same intrinsic firing property.	37
3.4	FFI circuit is activated by granule cells stimulation.	38
3.5	Target dependent plasticity of granule cell synapses	40
3.6	Depressing inhibitory synapses in FFI circuit	42
3.7	Simulation of FFI circuit	44
3.8	Simulation of FFI circuit with different combinations of dynamics synapses	45
3.9	Interneuron spike output dynamics follow its input synaptic dy- namics.	47
3.10	Inhibitory output driven by realistic firing pattern of SC under 50 Hz GC stimulation	49
3.11	Dendritic feed-forward inhibition recording	50
3.12	Silencing a single basket cell indicates phasic somatic inhibition. .	52
3.13	Phasic somatic inhibition	53

LIST OF FIGURES

3.14	Deletion of Munc13-3 enhances the paired-pulse facilitation at GC → BC synapse.	55
3.15	Somatic feed-forward inhibition is more facilitating in Munc13-3 knockout mice.	56
3.16	Spike output of Purkinje cell	57
4.1	The age dependence of the granule cell synaptic plasticity	62
4.2	Postsynaptic receptor saturation is the underlying mechanism for the depressing synapse.	63
4.3	Removal of receptor saturation and Munc13-3 deletion do not change the facilitation at GC → SC synapse.	64
4.4	Multivesicular release and postsynaptic receptor saturation work synergically to cause the synaptic depression in GC → BC synapses.	65

List of Tables

3.1	The steady-state level of inhibition	53
-----	--	----

LIST OF TABLES

1

Introduction

1.1 Part one: synaptic transmission

In 2008 I attended an IEEE workshop on the application of information theory in biology and other fields. I gave a short talk about information transmission through dynamic synapses which was my Master's thesis work. Since most of attendances of this workshop were electrical engineers or mathematicians, my talk drew some attention. Here is an interesting conversation between me and an engineer.

THE ENGINEER: You were saying a synapse works as a communication channel and I wonder how they are comparable?

ME: Physically a communication channel is an information transmission medium. The function of a channel is to convey messages from its senders to its receivers. A synapse in the nerve system consists of a presynaptic site, a postsynaptic site and the cleft between them, you see, like this (Fig. 1.1). It is shared by two neurons which are the sender and the receiver.

[I drew a cartoon (Fig. 1.1) on the blackboard behind me to illustrate a chemical synapse.]

1. INTRODUCTION

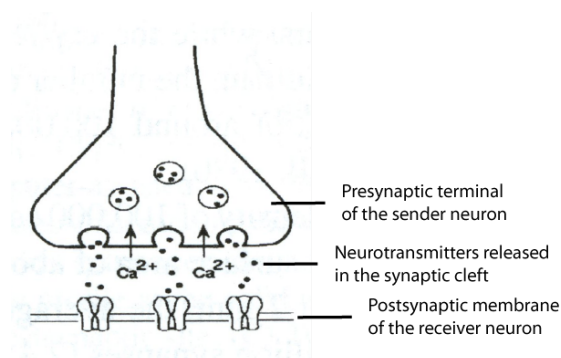


Figure 1.1: A cartoon of a chemical synapse - It shows a presynaptic terminal facing the postsynaptic membrane. Synaptic vesicles fuse with the presynaptic membrane upon Ca^{2+} entering into the presynaptic terminal, which leads to the release of the neurotransmitters to the synaptic cleft. The neurotransmitters diffuse across the synaptic cleft which is typically tens of nanometer wide, and bind to the postsynaptic receptors which are usually ligand-gated ion channels. The neurotransmitters are the media for information transmission across synapses. The information transmission is modulated by multiple factors from both the sender and the receiver neuron. Adapted from "Biophysics of Computation" (Koch, 1999).

ME: You might wonder how information is relayed through a synapse. Let's take this example of a chemical synapse. First, we ask what message a sender neuron wants to convey to a receiver neuron. The message could be a command "fire!" or the other way around "silence!". The message carried by action potentials (APs) generated at the soma of the sender neuron will travel along the axon of the neuron and reach the presynaptic terminal. Then the message will be encoded there and this code could be an ion concentration or the number of neurotransmitter molecules. The information carried by the code is then transmitted through neurotransmitters released from the presynaptic terminal to the synaptic cleft, as when you speak on one side of a telephone, your speech is carried by the electromagnetic waves traveling through the cable. Postsynaptic receptors are the receivers for this special code as the cable at the other side of the telephone. Once the code is received, the postsynaptic response can be observed as the change of the membrane potential. The process from presynaptic neurotransmitter release to the binding of postsynaptic recep-

1.1 Part one: synaptic transmission

tors is called synaptic transmission. Just before and after synaptic transmission there are encoding and decoding processes for the information conveyed through the communication channel - synapse. Putting them together, it is resembling a full communication system. The majority of the neuronal communication is mediated by chemical synapses through this type of synaptic transmission. One can evaluate the amount of information transmitted through a synapse as an engineer does this with a communication channel. Now, isn't it quite clear how a synapse is comparable with a communication channel?

THE ENGINEER: I agree that communication between neurons is indeed an information transmission process. Synapses represent physical communication channels as you pointed out. But how is the information quantified in terms of neurotransmitters and is there a physical model for the channel?

ME: You have asked the right question! To quantify the information and find out the right model for synaptic transmission has been an ongoing research topic for many years. Information can be quantified by the amount of neurotransmitters, but this variable is difficult to obtain through measurement during neuronal communication processes. Instead, the conventional neural code, the action potential, is much easier to monitor. Therefore it is natural to take the whole process, from presynaptic action potentials to postsynaptic action potentials, as a full information transmission channel, and the core of the problem is to find out a full description of the transmission process which involves neurotransmitter release and diffusion, postsynaptic receptor activation and the intrinsic electroresponsiveness of the postsynaptic neurons. In this whole process, multiple physical and chemical reactions are involved, each of which should be modeled in order to calculate the amount of information transmitted. Maybe we should take a detailed look at what is going on during synaptic transmission.

1. INTRODUCTION

[*The old man looked very interested, so I decided to tell him more about synaptic transmission.*]

ME: A synapse is activated by an action potential which depolarizes the membrane of the presynaptic terminal. Action potentials are usually stereotyped, therefore the amount of membrane potential change due to an action potential does not carry information about the activity of presynaptic neurons, rather the arrival time of the action potential and its presence or absence encode the signal. Depolarization activates voltage gated calcium channels on the membrane and leads an influx of Ca^{2+} ions into the presynaptic terminal. Ca^{2+} plays multiple roles in synaptic transmission (Neher and Sakaba, 2008). It triggers the cascade of synaptic vesicle fusion and it has been shown in many synapses that if no Ca enters in the presynaptic membrane, no vesicle will be released even when an action potential depolarizes the membrane (Mintz et al., 1995; Borst and Sakmann, 1996). The change of the presynaptic Ca^{2+} concentration signals the activity of the presynaptic neuron and the presynaptic Ca^{2+} concentration determines the vesicle release rate (Schneggenburger and Neher, 2000; Neher and Sakaba, 2008), therefore the information carried by the presynaptic $[Ca^{2+}]$ is transmitted to the neurotransmitter concentration in the synaptic cleft. Released neurotransmitters diffuse to the postsynaptic site, bind to receptors, and activate ion channels on the postsynaptic membrane. Neurotransmitters then passes the information to the change of postsynaptic membrane conductance due to the opening of receptor channels. The postsynaptic neuron then performs an inverse operation to generate from the change of the membrane conductance to action potential output. Empirically one can measure the input and output APs and calculate the information transfer rate or the channel capacity. At the same time, precise mathematical models are proposed to describe the process of synaptic transmission and analyze its properties (Schneggenburger and Neher, 2000; Millar et al., 2005; Pan and Zucker, 2009).

1.1 Part one: synaptic transmission

THE ENGINEER: Well, given how complex is the process you just described and how many times the information has been transformed within the whole process, I wonder how reliable is this information transmission process.

ME: Indeed, an individual synapse is not a reliable device due to the noise introduced in each step and most importantly the intrinsic stochasticity. First of all, a voltage gated ion channel opening is an all-or-none random process, and as shown experimentally (Patlak and Ortiz, 1986), the precise timing of a channel opening is a random occurrence. Second, a single vesicle release can be described as a binomial trial with a release probability p (Katz, 1969). Third, the amplitude of the postsynaptic response induced by a single vesicle release follows a near Gaussian distribution (Boyd and Martin, 1956). Besides, synapses undergo use-dependent modification, meaning that the synaptic parameters, like p or the mean amplitude of the Gaussian distribution, are dynamic variables during synaptic activities. All of these make the communication through a chemical synapse much less reliable than any electronic communication.

Whether the unreliability of synaptic transmission reflects a natural limitation of the biological device or it is part of the synaptic algorithm remains unclear. But the nervous system seems having its own way to compensate unreliability by increasing redundancy (Moore and Shannon, 1956), which is, for example, using parallel synaptic connections. From information point of view, higher variability presented in the synaptic variables indicates a higher capacitance for carrying information. Besides, there is a prominent view that synapses take advantages of their unreliability. The change of vesicle release probability p during ongoing activities, for example, is one possible advantage, which enables a dynamical modification of the synapse depending on the input activity. In this sense, the lack of reliability is required for

1. INTRODUCTION

a synapse to gain a larger dynamic range for information processing.

THE ENGINEER: That is an interesting view. In our field, we wish to design all the elements as constant as possible to avoid adaptation or any use-dependent effects. In fact, synapses may take advantages of their unreliability and use-dependent dynamics. If this property will be studied carefully, it might bring a completely new concept into the electronic system. Can you tell me more about the synaptic dynamics? What triggers the modification? Which parameter is modified? What is the time scale of the modification? How does it affect the function of a synapse?

ME: Biologists usually call this synaptic modification "plasticity". It is an adaptive behavior of the nervous system to inputs. It is often categorized into two types based on the timescales: long-term and short-term plasticity. Long-term synaptic plasticity (LTP) modifies the synapse in a time scale of hours or even longer. Short-term plasticity (STP) happens within milliseconds to seconds. The underlying mechanisms and functions of these two types of synaptic modification are different. Long-term synaptic plasticity has been studied quite a lot and it is speculated to underlie learning (Brown et al., 1990). Short-term synaptic plasticity exerts similar amount of change on the magnitude of postsynaptic responses as LTP, but in a much rapider form and more relevant to the information transmission through synapses. I am working on short-term plasticity, so let me answer your questions based on this type of synaptic modification.

1.2 Part two: Short-term synaptic plasticity (STP)

[I went on and presented the topics about short-term synaptic plasticity to the engineer who seemed quite fascinated by the adaptive behavior of a synapse.]

1.2 Part two: Short-term synaptic plasticity (STP)

ME: In nervous system short time scale modification occurs at all levels during neuronal activities, from ion channels and synapses to single neurons and neuronal circuits. The rapid adaptation of the nervous system is not only crucial because of the ever-changing environment with which it interacts, but also important for its computational functions (Abbott and Regehr, 2004) which enable information processing within milliseconds to seconds. Synaptic modification was first discovered in neuromuscular junction (Feng, 1941) where an enhancement of postsynaptic responses were observed during a prolonged stimulation of presynaptic neuron. Later, various dynamics have been found in a big number of synapses which are experimentally accessible (Zucker and Regehr, 2002).

THE ENGINEER: **How is the synaptic modification reflected in the postsynaptic responses and what are the different forms of short-term dynamics?**

ME: Synaptic dynamics reflected in the postsynaptic responses take basically two forms, enhancement and depression. During repetitive use of synapses, some synapses show increased postsynaptic responses, which is called short-term synaptic facilitation; and some show decreased postsynaptic responses, which is named short-term synaptic depression. In the other cases, the postsynaptic response can be first enhanced and then depressed during the activity, which implies that the facilitation and depression are intermingled and probably the sole facilitation or depression just shows the dominant side of the synaptic modification (Fig. 1.2).

As I mentioned before, synaptic transmission mainly involves three elements: presynaptic Ca^{2+} channels, synaptic vesicles and postsynaptic receptors. The short-term modification can happen to any of the three elements. From only the postsynaptic response, it is difficult to tell where the modification happened. Fortunately there are ex-

1. INTRODUCTION

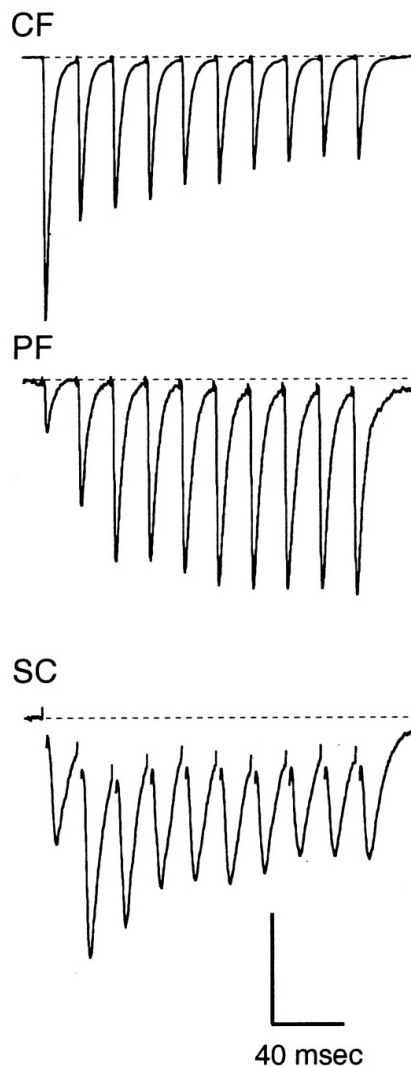


Figure 1.2: The different forms of short-term synaptic plasticity - The figure shows three different forms of short-term synaptic plasticity from three different synapses. Under a 50Hz train of presynaptic action potential stimulation (not shown), the postsynaptic responses from a climbing fiber (CF) synapse shows depression, those from a parallel fiber (PF) synapse shows facilitation and those from a Schaffer collateral (SC) synapse presents a transient facilitation followed by depression. (Adapted from (Dittman et al., 2000))

perimental techniques which enable us to observe the change of these synaptic elements separately. Presynaptic Ca^{2+} current measurement or Ca^{2+} -sensitive dye imaging reveals the change of the amount of

1.2 Part two: Short-term synaptic plasticity (STP)

Ca^{2+} entering the presynaptic terminal during the activity (Yuste and Konnerth, 2005). Presynaptic capacitance measurement helps to calculate how many vesicles are released upon each action potential invading the presynaptic terminal. Applying neurotransmitter agonist or antagonist to the synaptic cleft usually reveals the effect of postsynaptic receptor desensitization (Jones and Westbrook, 1996; Trussell and Fischbach, 1989) or saturation (Tong and Jahr, 1994).

How these elements are modified and how much they are modified are quite synapse-specific. There are some general phenomenons which are shared by many types of synapses. The elevation of presynaptic $[\text{Ca}^{2+}]$ after synaptic activity has been observed in mammalian central and peripheral synapses and it correlates with the enhancement of the synaptic transmission (Delaney et al., 1989; Regehr et al., 1994; Kreitzer and Regehr, 2000). Increase of the vesicle release probability estimated from statistics of release has been proved to be the general mechanism of facilitation in postsynaptic responses (Zucker, 1989). According to the quantal model of synaptic transmission (Katz, 1969), following a presynaptic action potential, the postsynaptic response R can be described as

$$R = npq. \tag{1.1}$$

n is the number of release site, p is the release probability per site and q is the quantal response triggered by a single released vesicle. Any alteration of these three parameters will lead to the change of the amplitude of postsynaptic responses. One prevalent view of depression mechanism is related to p . p is a product of the probability of vesicle occupancy in each release site and the probability of vesicle release. The repetitive use of the synapse reduces the probability of synaptic vesicles docked on release sites because after release each release site needs seconds to minutes to be refilled (Varela et al., 1997). Saturation (Tong and Jahr, 1994) or desensitization (Jones and Westbrook, 1996; Trussell and Fischbach, 1989) of postsynaptic receptors

1. INTRODUCTION

can make the target neuron less sensitive to neurotransmitters and produce decreasing postsynaptic responses. Other factors can also contribute to the change in synaptic responses during activity, such as the release of modulatory substances from the activated presynaptic terminals, postsynaptic cells, or neighboring cells (Davies et al., 1990; Isaacson et al., 1993; Wu and Saggau, 1997; Zilberter et al., 1999). These modulators could influence the presynaptic Ca^{2+} channels or the postsynaptic receptors and further inhibit or activate synaptic transmission. From one synapse to another, the degree and the time scale of the modification also vary. Some synapses show moderate facilitation, while others can have 2-3 fold enhancement (Beierlein et al., 2007). Some synapses show facilitation only within 20-50 ms, while others can have enhancement lasting hundreds of milliseconds (Bao et al., 2010).

THE ENGINEER: Multiple mechanisms may happen at the same time for a single synapse. Is it possible to find a mathematical description of short-term plasticity without involving the detailed biophysical process underlying it?

ME: Yes, mathematical descriptions have been proposed as phenomenological models (Liley and North, 1953; Varela et al., 1997; Tsodyks and Markram, 1997). They focus on describing the dynamics of postsynaptic responses without involving the underlying mechanism. In the literature (Varela et al., 1997), a straightforward version of this kind of model was described and fitted to the experimental data. The model calculates the postsynaptic response R as a product of the initial response R_0 and several dynamic variables representing depression or facilitation, as

$$R = R_0 F D. \tag{1.2}$$

F is a facilitation factor which is constrained to be ≥ 1 . Upon each

1.2 Part two: Short-term synaptic plasticity (STP)

action potential triggered release, a constant, $f(\geq 0)$, representing the amount of facilitation due to this AP is added to F :

$$F = F + f. \quad (1.3)$$

Before the next action potential arrives, F recovers exponentially back to 1 with a time constant τ_F :

$$\tau_F \frac{dF}{dt} = 1 - F. \quad (1.4)$$

Dynamic variable D is representing depression and it is constrained to be ≤ 1 . After each action potential triggered release event, D is multiplied by a constant, d , representing the amount of depression:

$$D = Dd. \quad (1.5)$$

Between APs, D recovers exponentially back to 1 with a time constant τ_D :

$$\tau_D \frac{dD}{dt} = 1 - D. \quad (1.6)$$

Since multiple factors underlie short-term synaptic plasticity, one or two processes may not be good enough to predict synaptic responses upon repetitive inputs. It is possible to add more dynamic variables to the model, for example,

$$R = R_0 F D_1 D_2. \quad (1.7)$$

D_1 and D_2 are independent variables and each has its own parameter set, $\{d, \tau_D\}$. Finding the best fit to the experimental data allows to tell which model is more precise.

There are other variants of this FD model. For example, a model incorporates Ca^{2+} dependent facilitation and recovery (Dittman et al., 2000) which introduces variables as occupancy of release sites by Ca^{2+} -bound molecules CaX_F and CaX_D . CaX_F will experience a

1. INTRODUCTION

jump of size Δ_F and CaX_D with Δ_D after an action potential at time t_{sp} . After the jump, they both decay exponentially back to 0 with first-order dynamics:

$$\frac{dCaX_F}{dt} = \frac{-CaX_F(t)}{\tau_F} + \Delta_F \cdot \delta(t - t_{sp}) \quad (1.8)$$

$$\frac{dCaX_D}{dt} = \frac{-CaX_D(t)}{\tau_D} + \Delta_D \cdot \delta(t - t_{sp}) \quad (1.9)$$

The facilitation variable F and the depression variable D as in the simple phenomenological model (Varela et al., 1997) will depend on CaX_F and CaX_D .

Another phenomenological model has been proposed based on the vesicle pool depletion model (Liley and North, 1953) and dynamics of vesicle release probability p_r (Tsodyks and Markram, 1997; Markram et al., 1998). The postsynaptic response A is the product of R (the fraction of occupied release sites), p_r and q (quantal size),

$$A = Rp_rq \quad (1.10)$$

similar to Eq.1.1. But here the total number of release sites is normalized to 1 and the release probability per release site p in Eq. 1.1 is represented by the production of R and p_r . The depletion model is described by dynamics of R :

$$\frac{dR}{dt} = \frac{1 - R}{\tau_r} - R \cdot p_r \cdot \delta(t - t_{sp}). \quad (1.11)$$

The R dynamics is similar as Eq. 1.9. When a presynaptic AP arrives at time t_{sp} and it triggers a release event, R decreases by the number $R \cdot p_r$. After this release, R recovers exponentially to 1 with time constant τ_r . The R dynamics accounts for the depression, and facilitation is described by p_r dynamics with a similar first-order differential

1.3 Part three: The Computational function of STP

equation:

$$\frac{dp_r}{dt} = -\frac{p_r}{\tau_f} + p_0 \cdot (1 - p_r) \cdot \delta(t - t_{sp}). \quad (1.12)$$

p_0 is the initial release probability. An action potential will induce an increase of p_r by $p_0 \cdot (1 - p_r)$ and p_r decays to 0 with a time constant τ_f during inter-spike intervals. This is different from the FD model and the Ca^{2+} -bound molecule model. In those two models, the facilitation variable has a fixed increase upon each action potential. Another difference between this "R - p_r " dynamics model with the other two models is that R dynamics is also a function of p_r (Eq. 1.11), where in the FD model and the CaX dynamics model, depression and facilitation variables are independent.

1.3 Part three: The Computational function of STP

THE ENGINEER: What I have learned today is that a synapse is a communication channel between two neurons and it is not passively and faithfully transmitting signals, rather it actively governs and modulates the flow of information between neurons. From all the biological facts which give rise to the privileged position of a synapse in the nervous system, and especially from the rapid dynamics of a synapse, one would easily predict that a synapse is not only a communication channel but rather importantly a computational unit. I wonder how much people have learned about the algorithms of a synapse.

ME: Traditionally, synapses were seen as a relay station of information between neurons. The specific pattern of connectivity, variable strengths and dynamics, make it obvious that synapses also support a variety of

1. INTRODUCTION

information processing algorithms and computations. In a neuronal circuit, the increase of the number and the variability of synapses enhances the computational capacity of the circuit. In the whole brain, an enormous number of synapses, approximately in the order of 10^8 per cubic millimeter, construct the architecture of the neuronal communication and computation.

The algorithms of synapses have not yet been identified completely due to the broad variation of synapses and the difficulty of accessing them experimentally, although a number of functional roles have been proposed for short-term synaptic plasticity (Dittman et al., 2000; Tsodyks and Markram, 1997; Fuhrmann et al., 2002; Abbott and Regehr, 2004; Silberberg et al., 2004; Abbott et al., 1997; Markram et al., 1998; Maass and Markram, 2002; Fortune and Rose, 2002; Goldman et al., 2002; Lisman, 1997).

STP as a temporal filter

The amplitude and the timing of the postsynaptic responses will influence the generation of postsynaptic action potentials. Synaptic plasticity regulates the amplitude of postsynaptic responses and further influences the responsiveness of the postsynaptic neuron to the presynaptic action potential. If a synapse without plasticity receives suprathreshold synaptic inputs, the output action potential will follow exactly the presynaptic action potential and this synapse works as a simple relay between neurons. With synaptic plasticity, synapses can filter the presynaptic input and govern the temporal structure of the postsynaptic output (Dittman et al., 2000; Silberberg et al., 2004; Fortune and Rose, 2002; Lisman, 1997; Chance et al., 1998). For example, a depressing synapse transmits lower frequency inputs better than higher frequency ones because high frequency presynaptic APs will deplete the vesicle pool faster and the postsynaptic neuron can not follow the activity of the presynaptic neuron. A facilitating synapse

1.3 Part three: The Computational function of STP

may follow high frequency inputs better than lower frequency ones. Facilitating synapses usually have low initial release probability and the synaptic strength is weak. High frequency inputs accelerate the accumulation of presynaptic Ca^{2+} and increase the synaptic strength (Borst and Sakmann, 1998). Therefore the postsynaptic neuron is driven from a nonresponsive state to a responsive one following the high frequency activity of the presynaptic neuron, while low frequency inputs may not facilitate the synaptic strength enough to trigger the response of the postsynaptic neurons.

The temporal filtering property of a synapse is not fixed. Depending on the state of the neuron or the modulation it receives, the release probability or the recovery rate of vesicles can be changed during activities (Zucker, 1973; Dittman and Regehr, 1998; Wang and Kaczmarek, 1998; Stevens and Wesseling, 1998). If the synaptic parameters are modified, an original depressing synapse may behave more facilitating and vice versa, so the filtering parameter of a synapse is also a dynamic variable.

STP enhances transient input

One important function of nervous system is to respond to the changing of the environment. Neurons typically respond most effectively to new stimuli and show adaptation to static input. Synaptic depression serves as one of the mechanisms for the adaptation. When a train of APs arrives at the presynaptic terminal, only the onset of the input elicits a large postsynaptic response due to the synaptic depression, and the postsynaptic neuron will be either excited or inhibited transiently depending on the type of neurotransmitter it receives. This function also correlates with the notion that information is encoded in the onset of a stimulus (Thorpe et al., 2001; Foffani et al., 2009). Some of the depressing synapses show transient facilitation when the frequency of presynaptic AP suddenly increases,

1. INTRODUCTION

and the transient facilitation accounts for a mechanism of enhancing the responsiveness of the postsynaptic neuron to the change of the temporal structure of the stimuli.

STP transmits history-dependent information

Synaptic plasticity comes from various modulations of synaptic parameters during repetitive use of the synapse. Information transmitted through a dynamic synapse contains the history of the presynaptic neuronal activity which has been successfully quantified through information theory (Fuhrmann et al., 2002). Synaptic plasticity assures that the current activity of a neuron reflects both the current state and the history of its input. Depression and facilitation differ on how much information about the history is transmitted.

STP as a gain modulator

Depressing synapses modulate the gain of synaptic responses dynamically by increasing the sensitivity of neurons to the relative changes of the input frequency. This function has been brought about by pure mathematical analysis of synaptic depression. Experimental evidences showed that the magnitude of postsynaptic responses is the largest upon the first spike input and then decreases until reaching a steady-state. The relative synaptic strength of the steady-state per presynaptic AP ($A = A_i/A_1$) is inversely proportional to the frequency (f) of the input spikes (Abbott et al., 1997):

$$A(f) \approx \frac{C}{f}. \quad (1.13)$$

C is a constant varying from a synapse to another. Then the postsynaptic response per unit time is

$$f \times A(f) \approx f \times \frac{C}{f} \approx C. \quad (1.14)$$

1.3 Part three: The Computational function of STP

It is obvious that the steady-state postsynaptic response per unit time is independent of the input spike frequency. The loss of the sensitivity to the input frequency is accompanied by an increase of the sensitivity to the relative change of the frequency ($\Delta f/f$) which can be deduced this way: when an abrupt change in firing rate of the presynaptic neuron happens, the instantaneous postsynaptic response is

$$\Delta f \times A(f) \approx C \frac{\Delta f}{f}. \quad (1.15)$$

This produces the transient change in the postsynaptic response proportional to the relative change in the firing frequency, which renders the synapse to detect small changes in the input frequency for slow input. This gain control mechanism of depressing synapses is similar to the Weber-Fechner law described in the human sensory system.

THE ENGINEER: It looks like a dynamic synapse could play different roles in different systems. Since the dynamic form of a synapse can be modified during activities, its functional role may be also possible to switch from circuit to circuit, like the resistors and capacitors in an electronic circuit. Depending on how you connect them, an integrator can be turned to a differentiator. Then it would be more desirable to study the function of a dynamic synapse inside a specific neuronal circuit.

ME: That is exactly what I am trying to do now! There are many types of neuronal circuits in the brain depending on the types of neurons, the types of synapses and their connectivity patterns. The same dynamic synapses may play different roles when they are connected differently. The circuit dynamics depend on the neurons, their connecting synapses and the interaction between them. In order to understand how much a dynamic synapse is participating in the circuit

1. INTRODUCTION

information processing, one has to find out the relationship between the circuit dynamics and the synaptic dynamics. My objective is to find out how the circuit dynamics depends on the synaptic dynamics. If I can alter only one synaptic parameter in the neuronal circuit and leave others unchanged, then I can plot the relationship between the circuit output dynamics and that synaptic parameter. Unfortunately, it is not easy to alter only one synaptic parameter in a real neuronal circuit. But I was lucky because my supervisor suggested me to study a feed-forward inhibitory circuit in the cerebellum and it turned out that there existed two circuits which differed only on one synaptic parameter. What I had to do is to find experimental approaches of measuring the circuit output and compare between the two circuits.

THE ENGINEER: Then I am looking forward to hearing about your results and by the way I could only suggest you to try computer simulations with the models of dynamic synapses which you just described to me. If you can simulate a neuronal circuit and compare with your experimental findings, I am sure you will gain some insights on the properties of both the circuit and the model.

[The end]

2

Materials & Methods

To investigate the short-term synaptic plasticity, electrophysiology recording is applied to exert a real-time control of the cell membrane potential and record the synaptic conductance change over time. Acute brain slice is an ideal preparation for studying neuronal circuits because substantial local neuronal connections are maintained within a thick slice. Whole cell patch clamp recording in acute brain slice is the fundamental experimental method for carrying out the study of the role of short-term synaptic plasticity in neuronal circuits. Dynamic clamp is an extension of patch clamp recordings to simulate artificial conductances in acute brain slices. Computer simulations can be used to simulate model circuits with artificial dynamics synapses.

2.1 Cellular organization of cerebellar cortex

The whole cerebellar cortex shares stereotypical organization which is composed of three layers: the granule cell layer, Purkinje cell layer and the molecular layer (Fig. 2.1). The cell types found in each layer and the connections between them are also similar throughout the cerebellum. The region called cerebellar vermis is located around the midline of cerebellum between two hemispheres. The cerebellar cortex in vermis receives spinal afferent through mossy fibers, and the output projects to deep cerebellar nuclei through Purkinje cell axons. The three layers of

2. MATERIALS & METHODS

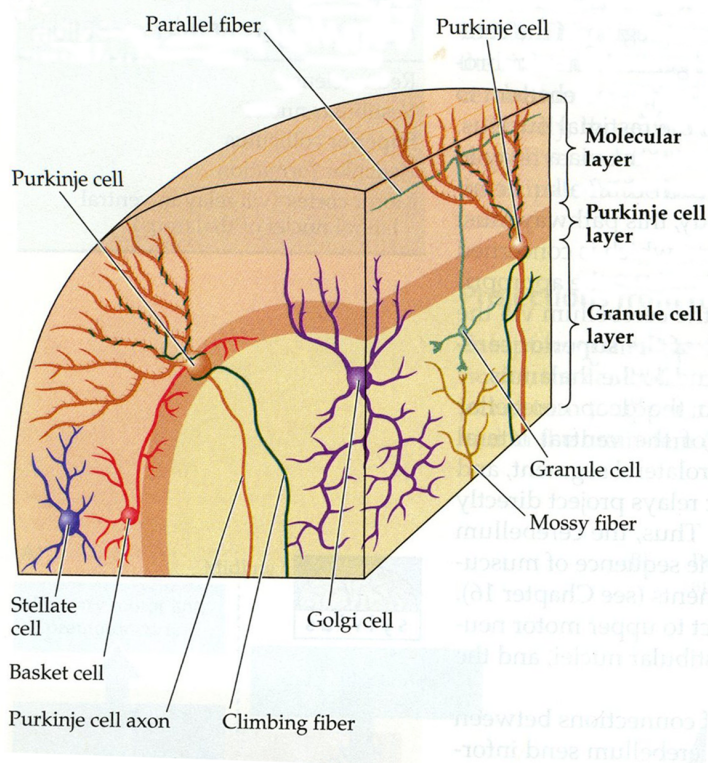


Figure 2.1: Three-layer organization of the cerebellar cortex - Adapted from "Neuroscience" (Purves et al., 2001).

the cortex have not only clear borders between each other, but also clear cellular connections. The granule cell layer, the first layer from the inner cortex to the pia, hosts mainly granule cells which send their axons - parallel fibers (PFs) - up towards the pia, pass the Purkinje cell layer and enter the molecular layer. The axon bifurcates in the molecular layer to two directions and runs a few millimeters in each direction making synaptic contacts with dendrites of Purkinje cells and molecular layer interneurons (MLIs). Purkinje cell layer is the second layer after the granule cell layer and it is a monolayered layer which looks like a natural border between the granule cell layer and the molecular layer. In the molecular layer, the cell density is very low and mainly interneurons are sitting there. The majority of the volume in the molecular layer is filled by the axons of granule

cells and dendrites of Purkinje cells and interneurons. Two types of interneurons are classified in the molecular layer. One is basket cell, located close to the Purkinje cell layer, and it makes basket-like synaptic terminals around the Purkinje cell soma. The other is stellate cell, located in the middle to outer layer of the molecular layer, and it innervates the dendrite of Purkinje cells. The granule cell \rightarrow MLIs \rightarrow Purkinje cell connections constitute feed-forward inhibitory (FFI) circuits in the cerebellar cortex. There is another type of cell, Golgi cell, which makes feed-back inhibition in the cerebellar cortex. Golgi cells sit in the granule cell layer and their dendrites spread into the molecular layer. Golgi cells receive inputs from granule cells and send inhibitory outputs to granule cells. Besides the major connections just described, there are also other contacts between cells in the cerebellar cortex. MLIs inhibit each other, and Purkinje cells also have synaptic contacts between each other.

2.2 Acute brain slice preparation

C57/Bl6N male and female mice (P16-P28) were decapitated in accordance with the guidelines of the German law on animal protection. This mouse line was chosen because of the availability of various knockout strains. Knockout mice provide a tool for studying neuronal circuits with altered parameters. After careful removal of the skull, the cerebellum and the brain stem were separated from the neocortex (Fig. 2.2). Coronal or parasagittal brain slices ($250\ \mu\text{m}$) of cerebellar vermis were obtained with a Leica VT1000S slicer (Leica Microsystems). During slicing the cerebellum was kept in ice cold solution containing (in mM) 60 NaCl, 120 sucrose, 25 NaHCO₃, 1.25 NaH₂PO₄, 2.5 KCl, 25 D-Glucose, 0.1 CaCl₂ and 3 MgCl₂ to minimize damage from anoxia and improve the texture of the tissue for slicing. The speed of the forwarding blade was set at the lowest level to prevent from stretching of surface neurons by the connecting tissues or neuronal fibers. Slices were incubated at 35°C in a saline solution (305 mmol/kg) containing (in mM) 125 NaCl, 2.5 KCl, 25 NaHCO₃, 1.25 NaH₂PO₄, 2 CaCl₂ and 1 MgCl₂, pH 7.3-7.4 with continuous bubbling (95% O₂ and 5% CO₂). This

2. MATERIALS & METHODS

was a critical step for recovering of the neurons from slicing. After 40 minutes to 1 hour recovery, the slice was moved to the recording chamber of about 1ml volume and fixed by a U-shape frame of metallic grid with parallel nylon threads. Recordings were performed at 33-34°C with a chamber heater and an in-line solution heater (Warner Instruments). Heated saline solution was perfused to the recording chamber at 2-3 ml/min. Continuous bubbling (95% O₂ and 5% CO₂) into the perfusion solution was necessary for keeping the pH value constant. Each slice can be recorded up to 1 hour depending on the neuron surviving situation. Due to the physiological recording temperature, neurons tend to deteriorate faster than recording under room temperature.

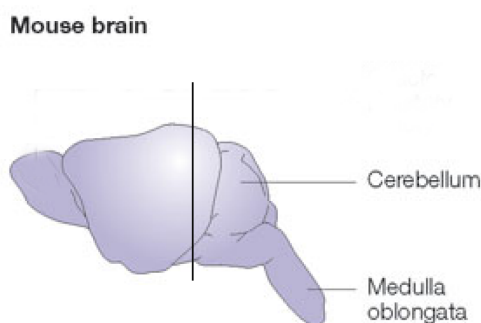


Figure 2.2: The mouse brain parasagittal view - The vertical line indicates the location where cerebellum and brain stem are separated from the neocortex during dissection process. The figure is adapted from the literature (Cryan and Holmes, 2005).

2.3 Slice patch clamp recording

2.3.1 Patch clamp recording setup

Slice patch clamp recording setup is made of three major parts: visualization, patch electrode and amplifier; with other auxiliary parts which surround or integrate into the major parts.

Cell visualization

Brain slices were visualized with an upright microscope (Olympus) using an oblique illumination technique, a condenser and high-numerical aperture water immersion objective (60 \times , Olympus). A CCD camera (TILL photonics) detected the light and converted it to an image on a monitor. When fluorescence imaging was used, we replaced the bright field illumination light source with appropriate monochromatic light generated from polychrome (TILL photonics) and inserted a filter between the objective and the CCD camera. The control program (Vision) supports specific time controlled imaging protocol to coordinate the camera and the polychrome.

The sample stage was fixed directly onto the antivibration table (Newport) to provide the best stability during recording. The microscope was mounted on a sliding table which enabled a two dimensional smooth movement relative to the sample stage. The micromanipulators (Linos) for holding and adjusting the patch pipettes were attached to columns which were mounted to the antivibration table. This configuration made sure that the relative position of the stage and the patch pipette did not change when adjusting the focus of the microscope or changing the field of view in the slice. Chamber heating device, the ground electrode and the suction pipe were fixed on the sample stage. Avoiding any touching between the stage and the microscope was important.

Amplifier and data acquisition

The amplifier EPC10 (Heka) was an all-in-one black box with data acquisition hardware together. The probe provided a pre-amplification which was directly connected to the patch pipette. Capacitance cancellation and series resistance compensation were done by the circuits on the main board of the amplifier. The Windows based control software patchmaster (Heka) provided an interactive interface for the user to either select automatic compensation or choose compensation parameters manually and visualize the results. The recording mode included voltage clamp and current clamp. In either case, data were filtered by an ana-

2. MATERIALS & METHODS

logue filter (10 KHz Bessel; current recordings were filtered additionally by 2.9 KHz Bessel filter.) in the circuits and sampled from 20 KHz to 50 KHz. There was a digital oscilloscope imbedded in the control software, so the real-time voltage or current traces could be visualized on the monitor. Data storage was also done by this software. Experiments were programed in a protocol file to enable automatic runs of different conditions and repetitions. The amplifier sent triggers to other hardwares coordinating the time sequence of different experiments.

2.3.2 How to identify a healthy neuron in the slice

Thanks to oblique illumination technique, neurons are having three dimensional appearance under the microscope. The edges of a neuron is especially distinct from supporting tissues around them. A healthy neuron should have smooth edges appearance. The cell surface should look bright and clean. If a cell looks either flat or dirty on the surface, it is a sign that it starts to deteriorate. It is easier to patch a neuron on the surface of the slice than in the deeper layer, so surface neurons should be taken as the priority for recordings. Finding a healthy neuron is the first step towards a successful patch clamp recording. If no healthy neuron can be identified from a slice, sometimes simply flipping the slice will help.

2.3.3 Whole-cell patch clamp of a neuron in the slice

Neurons in the slice were usually covered by a layer of tissues which tended to contaminate the tip of the glass pipette before it reached the surface of the neuron. A clean tip was essential for the pipette to form high-resistance seals with the cell, so a continually strong positive pressure should be applied to the patch pipette as it was advanced through the slice. The deeper the target neuron was, the stronger the positive pressure should be applied. Typically, pressures from 10 to 20 *mbar* were used for pipettes with a few $M\Omega$ resistance. Pressure was applied through a latex pipe connected to the patch pipette and it could be held

2.3 Slice patch clamp recording

by closing a valve. The level of pressure was monitored by a custom-made pressure sensor. Once the pipette tip was touching the membrane of the cell, which could be identified through a displacement of the cell or a bubble appearance on the surface of the cell, the positive pressure should be released immediately and a slight negative pressure (-10 mbar) was applied and held until a high-resistance seal was formed. Hyperpolarization of the patch pipette by 60 mV usually helped the seal formation.

Once the seal was formed, a very small amount of current ($\leq 10\text{ pA}$) should be flowing through the pipette in response to a 5 mV test pulse. Negative pressure should be released immediately, otherwise more membrane would be sucked into the pipette tip, which brought difficulty to the rupture process. Pipette capacitance should be canceled at this moment. Rupture of the patch membrane to obtain a whole-cell recording configuration was made by applying a brief pulse of suction to the patch pipette. After formation of a whole-cell configuration, the membrane capacitance and the series resistance (R_s) were estimated from the current response to a 5 mV test pulse. If the series resistance was too high ($\geq 10\text{ M}\Omega$ for a 3 – 4 $\text{ M}\Omega$ open pipette tip resistance, or $\geq 20\text{ M}\Omega$ for a 5 – 6 $\text{ M}\Omega$ pipette), a gentle suction were applied to open further the patch membrane. Once the series resistance was stable, membrane capacitance cancelation and series resistance compensation were applied.

Glass pipettes open tip resistances were 3-4 $\text{M}\Omega$ for big neurons ($\varnothing > 10\mu\text{m}$) and 5-6 $\text{M}\Omega$ for small neurons ($\varnothing \leq 10\mu\text{m}$). For voltage clamp experiments, the internal solution contained (in mM) 135 Cs-gluconate, 5 CsCl, 5 QX314 (chloride salt) (Tocris), 10 Hepes, 5 MgATP, 0.5 NaGTP and 1 EGTA, pH 7.2 and 310 mOsm. The junction potential was estimated to be 10mV from the reversal potential of the AMPA receptor current triggered by an excitatory synaptic input. The reported voltages in this thesis were not corrected for the junction potential. EPSCs were recorded in the presence of the selective GABA_A receptor antagonist SR 95531 (Sigma) at a holding potential of -65 mV. R_s compensation parameters were selected manually. For big cells like Purkinje cells, >60% of R_s was compensated, leaving <4 $\text{M}\Omega$ uncompensated series resistance. For small cells like

2. MATERIALS & METHODS

interneurons, the uncompensated R_s was $<10\text{ M}\Omega$. Current clamp experiments were performed with an internal solution containing (in mM) 135 K-gluconate, 10 KCl, 10 Hepes, 5 MgATP, 0.5 NaGTP and 0.1 EGTA. Usually the injected baseline current was 0 A, but in the case of a leaky cell, a certain amount of current was injected to compensate the leaky current and keep the cell in the resting state.

2.3.4 Dendritic patch clamp recording

To obtain patch clamp recording from dendrites, the basic procedure was the same as described in Sec. 2.3.3. However, it was facilitated by visualizing the dendrite through fluorescence dyes. Alexa 488 was dialyzed from a somatic patch pipette and after a few minutes even the finest dendrites were visible. The patch pipette for dendritic recording should have small opening ($\sim 7 - 8\text{M}\Omega$ open tip resistance), which also resulted in a high series resistance ($\sim 30\text{M}\Omega$). When approaching the dendritic membrane with the pipette, advancing from the top was easier than advancing from the side, because the dendrite of Purkinje cell was very thin on the z -axis ($\sim 2\mu\text{m}$) and the misalignment between the dendrite and the pipette tip would fail the seal formation. When advancing the pipette from the top, the displacement of the dendrite was observed due to the touching of the membrane by the pipette. Release of the positive pressure and immediately applying a small negative pressure ($\leq 10\text{mbar}$) at this moment gave a $\sim 50\%$ success rate for formation of $G\Omega$ seal. Voltage clamp from the dendritic patch pipette was almost impossible because of the high access resistance of the pipette and the high axial resistance within the dendritic tree. Current clamp were used to record the voltage change under the patch membrane.

2.3.5 Simultaneous multi-neuron recording

Simultaneous patch clamp recording from two or three connected neurons required careful handling of multiple pipettes in the restricted area. After finding the target neurons, it was better to insert all the pipettes before start approaching one of them. Usually one should patch the bigger neuron first and then the smaller one because with time the intracellular substance will be washed out by the pipette solution and the bigger cell can keep longer its own intracellular solution than the smaller cell. In the experiments studying inhibitory synapses, 5 mM GABA was included into the pipette solution. The successful rate of a pair recording was about 50% for basket cell and Purkinje cell pair and lower for stellate cell and Purkinje cell pair.

2.4 Extracellular stimulation

Extracellular stimulation was performed by inserting the tip of a glass pipette filled with saline solution into the granule cell layer. A very short (20-100 μs) voltage pulse was applied through the electrode inside the pipette to the slice. One can use either bipolar stimulation or unipolar stimulation. Bipolar stimulation was made of two electrodes closely placed around the stimulation pipette, either through a theta tube or simply wiring one electrode around the glass pipette. The advantage of bipolar stimulation was that the injected current was restricted at local area, which avoided the direct stimulation of a patch clamp recorded cell and also reduced the artifact picked by the patch pipette. Sometimes the stimulation intensity delivered by the bipolar stimulation was too small to excite enough cells for having recordable signal. In this case unipolar stimulation was necessary, although the drawback was that the ground electrode in the slice chamber was shared by the stimulation circuit and the injected current was spreading through the entire slice. Fortunately, the amplitude of the injected current decayed with distance in the brain slice. When the patch clamped cell was far from the stimulation place, unipolar stimulation was unlikely to stimulate directly the

2. MATERIALS & METHODS

recorded cell. For coronal slices stimulation pipettes were placed 100-200 μm from the recorded cell soma along the direction of the parallel fiber. In parasagittal slices, parallel fibers ran perpendicular to the slice surface; therefore stimulation pipettes were placed relatively close to the recorded cells. Stimulation intensity was adjusted to elicit small, but reliable postsynaptic responses.

2.5 Dynamic clamp

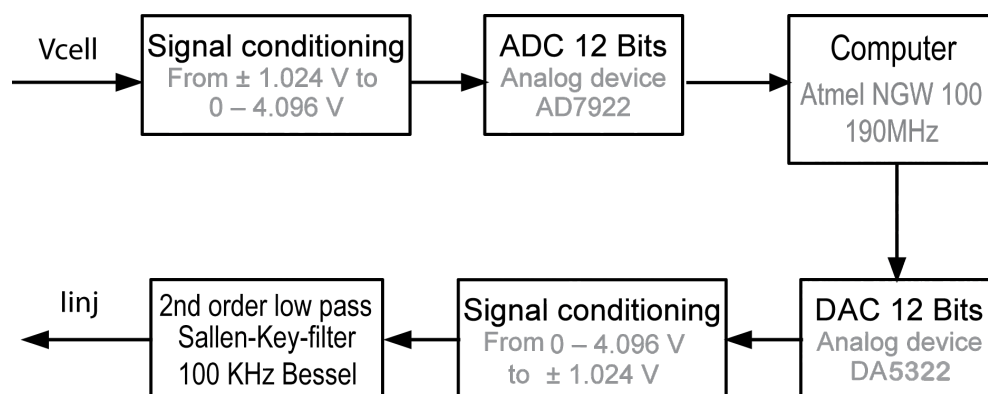


Figure 2.3: The hardware design of the dynamic clamp - The dynamic clamp device is a separate hardware from the electrophysiology experiment setup with its own computer for calculating online the injected current. The cell membrane voltage signal V_{cell} from the patch clamp amplifier is fed into the dynamic clamp as an input. After conditioning and AD conversion, the computer will calculate the current from V_{cell} and a conductance value read from a look-up table created beforehand or calculated online. The calculated current I_{inj} will be fed into a DA converter, a signal conditioning and a filter. The output from the filter will be fed into the external stimulation input channel of the patch clamp amplifier. The cycle length of the dynamic clamp can be set according to the sampling rate of the amplifier. Within each cycle, a voltage value is read and a current is injected to the cell through the same patch pipette. This device is designed together by Jin Bao and Frank Würriehausen, and manufactured by Frank Köhne.

Dynamic clamp is a device which can introduce artificial conductances into a real neuron during a conventional patch clamp experiment (Prinz et al., 2004). It can simulate various membrane conductances and inject the amount of current which

is calculated from the conductance and the real-time cell membrane potential. It has several forms of realization from analog device based version to Windows based version. Windows based version is easy to implement and has user-friendly interface, but it suffers from unexpected interrupts during the experiment, which leads to a false real-time update of the artificial conductance. An analog device based dynamic clamp requires a little more effort in implementation, but it can be controlled precisely and the update speed can be higher than other realizations. The basic architecture of an analog dynamic clamp is shown in Fig. 2.3. The input of the dynamic clamp was connected to the voltage monitor of the patch clamp amplifier. The cell membrane voltage reading from each sampling cycle of the amplifier was fed into the dynamic clamp for calculating the amount of the current to be injected. Before reaching the computer of the dynamic clamp, the voltage signal had to be scaled by an analog circuit, called conditioning, to match the range of the AD converter. After being digitized, the voltage signal went into the computer, where a pre-calculated look-up table for an artificial conductance was stored. The computer calculated the current according to

$$I = g \cdot (V - E). \quad (2.1)$$

The conductance g was a time varying variable which was pre-calculated if it was voltage independent. In the case of a voltage dependent conductance, online calculation was required. V was the membrane potential measured from the patch clamp amplifier and E was the reversal potential for the simulated conductance. $(V - E)$ was the instantaneous driving force for the conductance g . The calculated current I passed a DA converter and an inverse conditioning to scale back to the voltage input range of the amplifier. Before feeding the signal to external stimulation input of the amplifier, low-pass filtering was necessary to round up the sharp steps in the current resulted from the DA converter. The dynamic clamp update rate was set to the sampling rate of the amplifier. In each cycle of the dynamic clamp experiment, a real-time membrane potential V was read through the patch pipette under current clamp recording mode and an updated I was fed into the cell through the same patch pipette. The control program was written in C (with development environment AVR32 Studio 2.5.0 and compiler

2. MATERIALS & METHODS

avr32-gcc 4.3.2).

2.6 Data analysis and computer simulations

2.6.1 Experimental data analysis

Electrophysiology recording data were filtered at 5-10 kHz and sampled at 50 kHz. Offline analysis was carried out by custom written programs using Igor Pro (Wavemetrics) and Matlab (MathWorks). Sweeps were repeated 10-20 times in the train stimulation experiment and were averaged within a given cell. Peak amplitudes were detected as a local minimum (or maximum) for each response after average across sweeps. In the case of a slow decay signal from the previous response superimposed with the current one, fitting of the previous decay to an exponential function was performed to offset the current response to retrieve the evolution of synaptic current activity. Steady-state values were calculated from the mean of the last 5-10 responses depending on the visually detected steady-state. Unpaired t-test was performed with $\alpha=0.05$.

2.6.2 Simulating the model circuit

To construct a model circuit, all the synapses and neurons within the circuit have to be modeled. In the FFI circuit, I modeled an excitatory synapse, a fast spiking interneuron and an inhibitory synapse. Stochastic simulation was introduced only in the synaptic level.

The model of STP

Phenomenological model is practical for simulation because of the relatively small number of free parameters in the model. I have introduced three phenomono-

2.6 Data analysis and computer simulations

logical models in the Section 1.2. The Tsodyks-Markram model (TM model) (Tsodyks and Markram, 1997; Markram et al., 1998) is the best of the three because the FD model (Varela et al., 1997) suffers from an unbound facilitation and the Ca^{2+} dependent model (Dittman et al., 2000) has too many parameters. By fitting the synaptic responses to TM model one can obtain a set of parameters: the initial release probability p , the recovery time constant τ_r , and the facilitation decay time constant τ_f . An average from all the cells recorded in the same condition were fitted together using the simplex algorithm. The fitting routine was repeated 500 to 1000 times and each time random initial values of the parameters were chosen for avoiding finding a local minimum of the residuals. Then the SSE (the summed square of errors) from each fit was compared and the best fit was chosen with the smallest SSE. The model describes the average behavior of the short-term synaptic plasticity across multiple synaptic boutons and multiple trials, therefore the parameters obtained from the fit indicate averaged synaptic parameters. For example, the release probability, it can be referred to the release probability of a single release site according to the quantal release model (Katz, 1969), but the parameter from TM model should be considered as an average probability from multiple synaptic boutons weighted by their synaptic weights w_i , as

$$p = \langle w_i p_i \rangle . \quad (2.2)$$

The simulation was based on the stochastic depletion model and the model synapse was simulated by a stochastic algorithm to generate post-synaptic responses for a given spike train input (Bao, 2007). The number of release sites was assumed to be 10 to 20 in both excitatory and inhibitory synapse. The number of activated parallel fibers were from 20 to 100. A linear summation of synaptic input was assumed and the synaptic inputs from all the activated parallel fibers were assumed to arrive at the same time. The simulated synaptic conductance took a stereotyped waveform described by an alpha function. Only the peak conductance was generated from the stochastic simulation of TM model. The synaptic current was then described as

$$I(t) = (V - V_E) \cdot \sum_i G_i(t). \quad (2.3)$$

2. MATERIALS & METHODS

V was the instantaneous membrane potential and V_E was the reversal potential for this conductance. Summation was across all the synaptic inputs triggered by the input spike.

The model of fast spiking neuron

Leaky integrate-and-fire (LIF) model was used to simulate the fast spiking interneuron in the model circuit. The LIF model is not a real spiking model, meaning it does not describe the detailed time course of an action potential, but it fits to the frequency-current ($f - I$) relationship of a real neuron often as well as a conductance-based spiking neuron model. LIF model wins over the conductance-based model by its limited number of parameters which describe a subthreshold domain of activity and a voltage threshold for spike generation. For the purpose of simulating the spike output dynamics as a result of synaptic inputs, LIF model is appropriate. The leaky integrate-and-fire model deals with subthreshold integration via a capacitance C and a leak resistance R (Fig. 2.4). The input current $I(t)$ comes either from synaptic inputs or intracellular electrode. The voltage trajectory of the integrator is described by a first-order differential equation

$$C \frac{dV}{dt} + \frac{V - V_L}{R} = I(t) \quad (2.4)$$

which can be derived from Kirchoff's law. V_L is the resting membrane potential or leak reversal potential. Once the membrane potential V reaches the threshold V_{th} for spike generation, a spike is triggered and the voltage is reset to the leak reversal potential. Since the shape of the action potential is not described by the model, a delta function $\delta(t - t_i)$ is used to indicate a spike. The effect of the absolute refractory period is taken into account in the LIF model by postulating a fixed duration t_{ref} after the spike generation. During this period, any input current is shunted and the membrane potential is kept at the resting potential V_L . The LIF model was first fitted to the $f - I$ curve obtained from recording of molecular layer interneurons according to the relation between the mean firing

2.6 Data analysis and computer simulations

frequency $\langle f \rangle$ and the amplitude of the injected step current I :

$$\langle f \rangle = \frac{1}{t_{ref} - \tau \ln(1 - V_{th}/IR)}. \quad (2.5)$$

τ was the product of R and C . Both R and C were measured experimentally. Fitting to Eq.2.5 gave r_{ref} and V_{th} . During simulations, Eq. 2.6.2 was solved numerically based on Runge-Kutta algorithm. The resulting $V(t)$ integrated within each sampling interval of $I(t)$ was compared with V_{th} , and once V passed V_{th} the time was recorded as the time of a spike output and V was set to V_L for a period of t_{ref} .

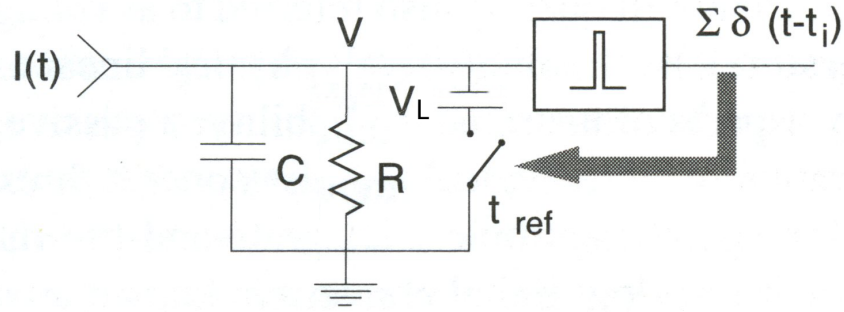


Figure 2.4: Leaky integrate-and-fire model - A subthreshold integrator within a single compartment described by a compound membrane capacitor C and resistor R . A leak reversal potential V_L is also known as resting potential. Spike generation is accounted by a delta function without describing the detailed time course. Once a spike is generated, any input $I(t)$ is shunted within an absolute refractory period t_{ref} and V equals to V_L . Modified from "Biophysics of Computation" (Koch, 1999).

2. MATERIALS & METHODS

3

Results

3.1 Cerebellar feed-forward inhibitory (FFI) circuits

To study how synaptic dynamics influence circuit dynamics, we have picked up an anatomically well defined microcircuit in the central nervous system - the cerebellar feed-forward inhibitory circuit. Feed-forward inhibitory circuit has two layers of information relay: an excitatory input to an inhibitory interneuron and the inhibitory output from that interneuron to a target neuron, see Fig. 3.1. The cerebellar feed-forward inhibitory circuit is transmitting information between granule cells (GC) and Purkinje cells (PC). It is composed of two different pathways: somatic FFI and dendritic FFI (Eccles et al., 1966a; Palay and Chan-Palay, 1974), see Fig. 3.2A. The cerebellar cortex is divided into three layers: the granule cell layer which is the input layer of FFI circuits; the molecular layer where interneurons are situated together with the axons of granule cells - parallel fibers (PF); and the Purkinje cell layer which is the output layer of FFI circuits. Parallel fiber terminals make glutamatergic synapses with PC and two types of interneurons, basket cell (BC) and stellate cell (SC). Basket cells make GABAergic synapses onto the soma of Purkinje cell, and stellate cells make GABAergic synapses onto the dendrite of Purkinje cell. Basket cell mediated somatic FFI circuit and stellate cell mediated dendritic FFI circuit share similar structure and common input from granule cells. The only differences between

3. RESULTS

them could be the input and output synapses in the circuit and the intrinsic firing property of interneurons. By comparing these two FFI circuits, the function of synaptic dynamics in the circuits may be revealed.



Figure 3.1: A cartoon of feed-forward inhibitory circuit - In the feed-forward inhibitory circuit, there are two layers of information relay: an excitatory input to the interneuron (IN) through input synapses and an inhibitory output to the target neuron through output synapses.

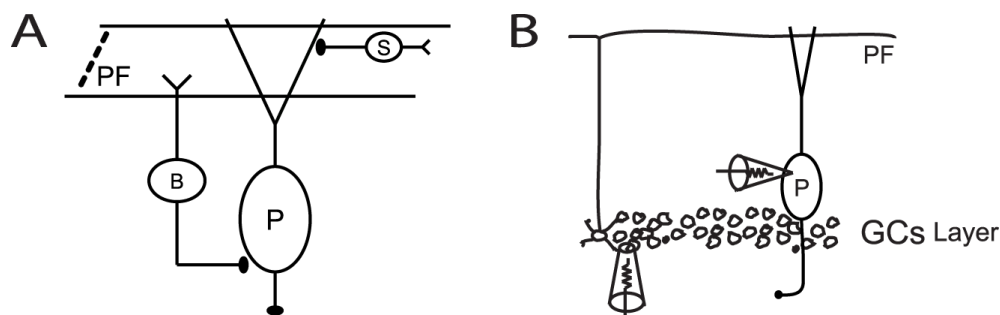


Figure 3.2: Cerebellar feed-forward inhibitory circuits - (A) Cerebellar feed-forward inhibitory circuits are composed of two pathways: basket cell mediated somatic inhibition and stellate cell mediated dendritic inhibition. They share common excitatory inputs from parallel fibers, the axons of granule cells. They target onto different subcellular compartments of Purkinje cell. (B) The experiment diagram of activating cerebellar FFI circuit. An extracellular stimulation pipette was placed into the granule cell layer and short voltage pulses were conveyed to depolarize granule cells. Patch clamp recording were performed in the circuit from either interneurons or Purkinje cells.

BCs and SCs share some morphological and physiological features (Sultan and Bower, 1998; Vincent and Marty, 1996) and protein expression (Kosaka et al., 1993; Caillard et al., 2000), while their firing properties have not yet been compared. I first characterized the intrinsic firing property of these two interneurons by injecting a steady current step to the cell soma and observing the output firing

3.1 Cerebellar feed-forward inhibitory (FFI) circuits

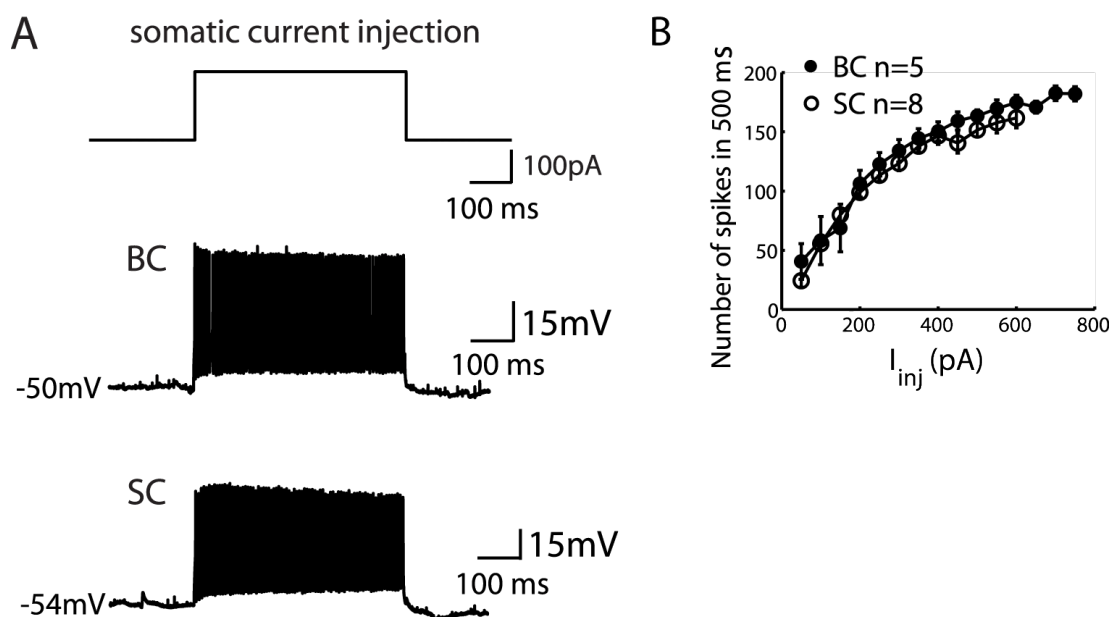


Figure 3.3: BC and SC share the same intrinsic firing property. - (A) A 500 ms, 200 pA current pulse was injected to the soma of BC and SC under current clamp recording mode. Responses from a BC and a SC are shown here. The example BC fired 140 Hz regular spikes and the SC fired 165 Hz regular spikes. The resting membrane potential of the BC is -50 mV and that of the SC is -54 mV. (B) Averaged spike counts within 500ms were plotted against the amplitudes of injected currents.

pattern. As shown in Fig. 3.3A, a 500 ms current pulse was injected into the soma under current clamp mode. BCs and SCs fired regularly without adaptation during constant current injection (an example from each cell type is shown and consistent results were observed in 5 BCs and 8 SCs). Their firing pattern can be classified as fast-spiking, which is commonly observed in inhibitory interneurons (Somogyi and Klausberger, 2005; Markram et al., 2004). The number of spikes was plotted against the amplitudes of injected current (shown in Fig. 3.3B), indicating that the intrinsic firing property of BC and SC were similar. Then the difference between somatic and dendritic FFI circuits may lie in the property of the input excitatory synapse and the output inhibitory synapse.

To further characterize the short-term synaptic plasticity and the circuit dynamics, inputs to the circuit were delivered by activating directly granule cells.

3. RESULTS

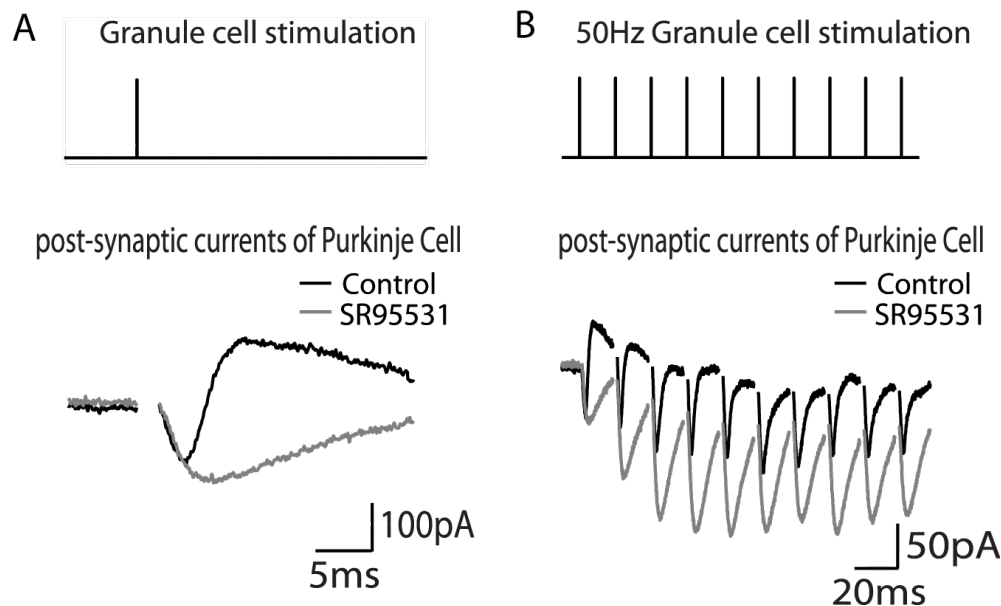


Figure 3.4: FFI circuit is activated by granule cells stimulation. - (A) A single extracellular stimulation applied to the granule cell layer elicited a post-synaptic current (PSC) recorded from the Purkinje cell soma. An excitatory current (negative) is followed by an inhibitory current (positive) in the control condition (black). GABA_A receptor antagonist SR 95531 blocks the inhibitory current (gray). Recorded cells were voltage clamped at -55 mV. Each trace is an average of 10 sweeps and stimulus artifacts are removed from PSC traces. (B) Trains of stimulation pulses were applied to the granule cell layer. An example of a 50 Hz train and its responses are shown in a similar way to A.

Extracellular stimulation was applied to GCs (Fig. 3.2B) rather than PFs in the molecular layer to avoid the direct stimulation of interneurons and the recruitment of more fibers during repetitive stimulations (Barbour, 1993; Marcaggi and Attwell, 2005; Beierlein et al., 2007). Patch clamp recordings were performed from Purkinje cells to record the output of FFI circuits. The stimulation strength was adjusted such that the amplitudes of postsynaptic responses were reliable and comparable to the ones in the previous studies (Barbour, 1993; Mittmann et al., 2005). The soma of the PC was voltage clamped and stimulations of GCs activated feed-forward inhibitory currents in the PC (Fig. 3.4). An excitatory inward current was followed by an outward current, which was blocked by the GABA_A receptor antagonist SR 95531, indicating a delayed disynaptic inhibition - feed-forward inhibition (Fig. 3.4A). During a 50 Hz train

3.2 Various forms of STP in the FFI circuit

of GC stimulation (Fig. 3.4B), both monosynaptic excitatory currents (from GCs) and di-synaptic inhibitory currents (from MLIs) observed at the PC soma showed short-term plasticity, implying that FFIs were dynamically recruited during activities. Specifically, the excitatory currents exhibited facilitation, while the inhibitory currents showed depression. How the synaptic dynamics in each layer of the circuit influence the output dynamics of FFI circuit is the main topic of this thesis.

3.2 Various forms of STP in the FFI circuit

Somatic and dendritic FFI circuit share the same input and the same firing property of the interneuron, while the properties of input and output synapse of the interneurons are unknown. By comparing the synaptic property of these two circuits, especially how these synapses are modified during ongoing activities, the function of synaptic dynamics in neuronal circuits can be studied.

3.2.1 Target-dependent STP of excitatory synapses

During repetitive stimulation synapses can exhibit different forms of short-term plasticity (Zucker and Regehr, 2002). To investigate the consequence of short-term synaptic plasticity on the circuit dynamics, I first examined the short-term plasticity of PF synapses formed by the GC axon terminals with PCs, BCs and SCs. To preserve PFs, experiments were performed on coronal slices. Trains of extracellular stimulation were applied to GCs with regular inter-stimulus intervals (ISIs) in the presence of a GABA_A receptor blocker. The evoked excitatory post-synaptic currents (EPSCs) were recorded from the target cells and 10 to 20 sweeps were averaged (Fig. 3.5A, B). Some experiments were performed with simultaneous voltage clamp recordings from PC and BC, as shown in Fig. 3.5A (top panel). EPSCs recorded from the PC showed strong facilitation during 50Hz-train stimu-

3. RESULTS

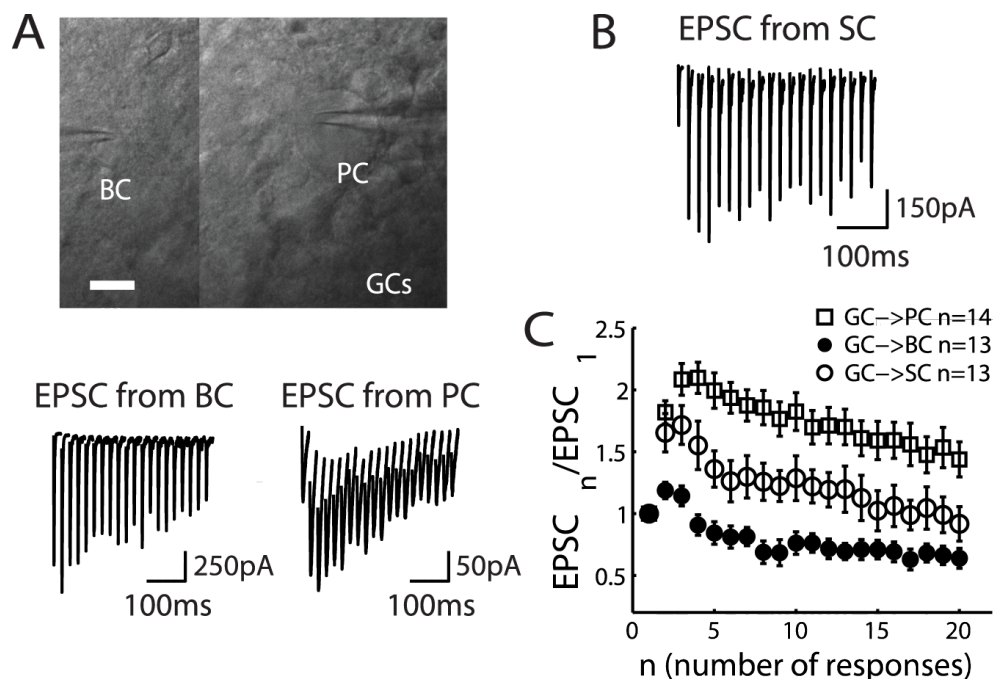


Figure 3.5: Target dependent plasticity of granule cell synapses - (A) Imaging of a simultaneous patch clamp recording from a Purkinje cell and a basket cell (scale bar is $10 \mu m$). EPSCs recorded from the BC upon 50 Hz GC stimulations are depressing and those recorded from the PC are facilitating. Cells were voltage clamped at -65 mV and in the presence of SR 95531. Each trace is an average of 10 sweeps. (B) EPSCs of a SC under the same experiment condition as in A. (C) Peak amplitudes of EPSCs recorded during the train are normalized to the first one and plotted against the number of responses. Each trace represents an average from 14 PCs (open square), 13 BCs (filled circle) and 13 SCs (open circle) (mean \pm s.e.m.).

lation (Fig. 3.5A bottom panel, right), consistent with previous studies (Barbour, 1993; Isope and Barbour, 2002; Dittman et al., 2000). The EPSC sizes were also comparable to the previous studies. In contrast, EPSCs recorded from the BC showed minor paired-pulse facilitation followed by a pronounced depression under the same stimulation condition (Fig. 3.5A bottom panel, left). EPSCs recorded at another type of interneuron, SC, showed strong facilitation, similar to GC \rightarrow PC synapses (Fig. 3.5B). In Fig. 3.5C, the peak amplitudes of EPSCs were divided by the first one in the train and plotted against the stimulus number (mean \pm s.e.m.), showing that PF synapses exhibited target-dependent short-term plasticity: GC \rightarrow PC and GC \rightarrow SC synapses are facilitating synapses, whereas GC

3.2 Various forms of STP in the FFI circuit

→ BC synapses are depressing synapses (comparing PC (n=14) and BC (n=13): $p < 0.0001$; comparing SC (n=13) and BC (n=13): $P < 0.05$).

3.2.2 Depressing inhibitory synapses

The excitatory input synapses present different forms of STP which filter the granule cells input according to the targeted interneuron. The signals coming to the interneurons will be further filtered by dynamics of inhibitory output synapses before reaching PCs. Different types of interneurons exhibit distinct short-term synaptic plasticity in neocortex and hippocampus (Beierlein et al., 2003; Hefft and Jonas, 2005), but a systematic comparison has not been made in the cerebellum. I therefore examined the dynamics of BC → PC and SC → PC synapses by simultaneous patch clamp recordings from a connected pair of cells. When a train of short current pulses was injected into the interneuron, spikes were elicited faithfully (Sakaba, 2008). The evoked inhibitory post-synaptic currents (IPSCs) were recorded from the PC using a pipette solution with 135 mM intracellular $[Cl^-]$ to amplify the inhibitory synaptic current by increasing the driving force for Cl^- ions. Fig. 3.6A shows averaged inhibitory current traces from 10 to 20 sweeps in response to a 50 Hz spike train. Both BC → PC and SC → PC synapses are depressed (n = 6 pairs of BC-PC, n = 4 pairs of SC-PC). The normalized IPSCs demonstrate that both synapses have similar short-term synaptic dynamics (Fig. 3.6B). However, we observed a 7-fold difference in their inhibitory strengths (BC → PC: 1.73 ± 0.55 nA; SC → PC: 0.24 ± 0.04 nA), which would be mostly due to the different size of the presynaptic terminals (Palay and Chan-Palay, 1974): the basket cell's axon forms a large terminal innervating the soma of a Purkinje cell, while the stellate cell contacts PC's dendrite through small synaptic buttons.

3. RESULTS

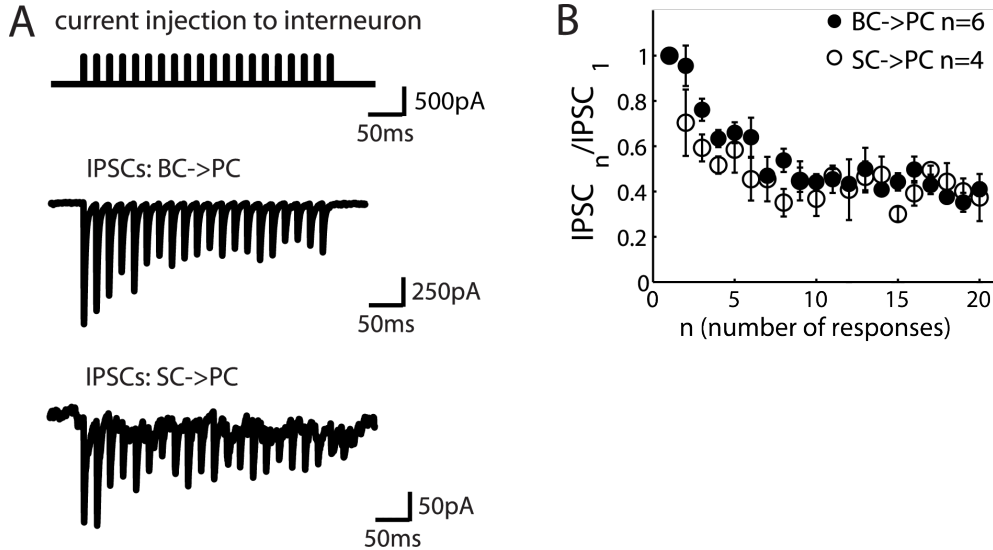


Figure 3.6: Depressing inhibitory synapses in FFI circuit - (A) 50 Hz current pulse injection to a BC or SC elicited a reliable spike upon each pulse (spikes were not shown). Simultaneous voltage clamp recording with 135 mM intracellular $[Cl^-]$ from a PC which is innervated by the interneuron shows inward inhibitory current (negative) with depressing dynamics. Holding potential was -70 mV. (B) Normalized IPSCs are plotted against the number of responses showing similar dynamics of these two synapses (mean \pm s.e.m.).

3.3 Interactions of STP in the FFI circuit

Information flowing through a FFI circuit will be filtered by an excitatory synapse and an inhibitory synapse in a row. Since the interneurons of the two FFI circuits share similar intrinsic firing property (Fig. 3.3), the difference between the output of the two circuits will mainly depend on the dynamics of their connecting synapses. Two depressing synapses are presented in the somatic FFI circuit, while a facilitating synapse and a depressing synapse coexist in the dendritic FFI circuit. STP only differs at the excitatory input synapse between somatic and dendritic FFI circuit. The difference of the output dynamics between these two FFI circuits was examined by both computational and experimental approaches to clarify the role of synapses in modulating the circuit dynamics.

3.3.1 Predicting circuit dynamics from a model circuit

A model circuit was constructed from an excitatory synapse, a fast spiking interneuron and an inhibitory synapse. The model of the excitatory synapses was stochastic TM model (Sec. 2.6.2) and the parameters were from fitting the EPSCs recorded from GC \rightarrow BC and GC \rightarrow SC synapses to the model. Interneurons were simulated with LIF unit (Sec. 2.6.2) with the same set of parameters for both BC and SC since they had similar $f-I$ curve (Fig. 3.3). 50 Hz regular spike inputs were delivered to the model circuit and the output spikes from interneurons were obtained and plotted as raster plots in Fig. 3.7. Through a depressing input synapse, the spike output of the interneuron followed the input only at the onset about 50-100 ms and afterwards the interneuron was almost silenced (Fig. 3.7A). When a facilitating synapse was the input synapse of the interneuron, persistent spike outputs were observed from the interneuron (Fig. 3.7B). Note that the initial spiking probability of interneurons in the two circuits were adjusted to be similar in the simulation. Inhibitory synapses were also simulated from stochastic TM model, and since BC \rightarrow PC and SC \rightarrow PC synapse share similar synaptic depression time course, the model parameters were taken from the fitted parameters of BC \rightarrow PC synapses for both circuits. The spike outputs of interneurons (raster plots in Fig. 3.7) were fed into the depressing inhibitory model synapses to generate the peak conductance of the synaptic output upon each spike. The summation of those peak conductances across 20 repetitions was plotted. The FFI circuit with two depressing synapses in series generated output only at the onset of each stimulus train (Fig. 3.7A, bottom panel) as a result of the phasic spike output of the interneuron. When a facilitating input synapse and a depressing output synapse were in series, the magnitude of the FFI circuit output first increased after the onset of the stimulus and then decreased to 60% of the initial amplitude at the end of the input (Fig. 3.7B, bottom panel). The depression seen in the circuit output is milder comparing with the depression of the inhibitory synapse in response to a regular spike train (Fig. 3.6) which has about 40% steady-state depression.

3. RESULTS

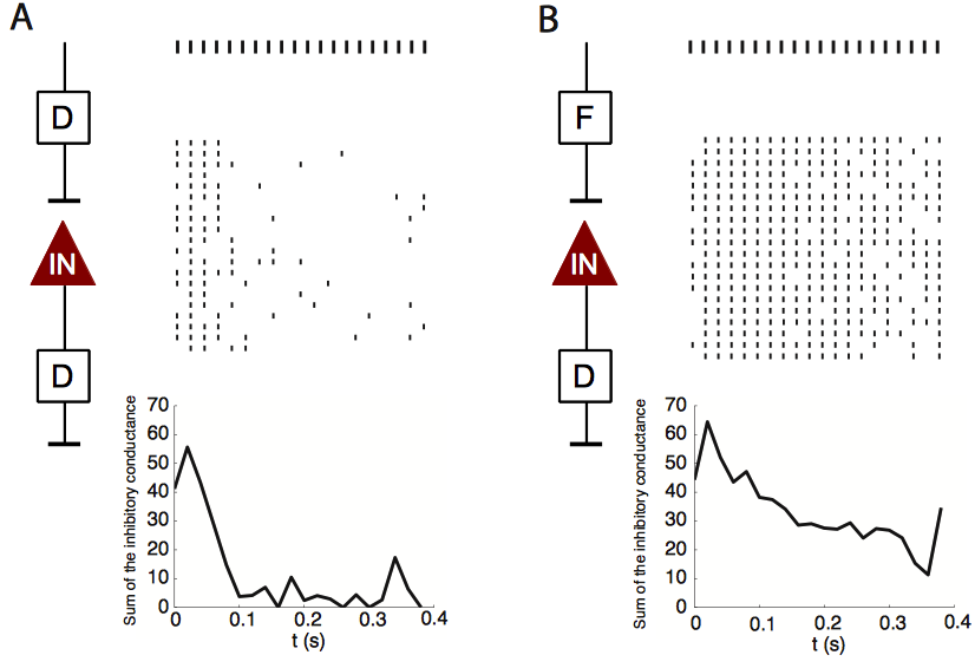


Figure 3.7: Simulation of FFI circuit - A regular train of action potential (50 Hz \times 20) was applied to the model circuit mimicking the GC input with 20 times repetition. Raster plots show the spike output of interneurons with depressing input synapse (A) and facilitating input synapse (B). The spike series were fed into the same depressing synapses for both circuits and the resulted inhibitory peak conductances were summed across 20 repetitions and plotted beneath the raster plots. The magnitudes of the conductance is a relative scale by assuming the quantal size of an inhibitory synapse is 1 in the simulation.

To further demonstrate the dependence of FFI circuit output on its input/output synaptic dynamics, different combinations of dynamic synapses have been plugged into the model circuit (Fig. 3.8). The circuit input was 50 Hz regular spike train as in Fig. 3.7 and hundreds of repetitions were applied. The resulted interneuron spike output is shown in Fig. 3.8A with a “F” indicating a facilitating input synapse in the circuit and a “D” for the depressing input synapse. Similar to Fig. 3.7, the facilitating input synapse drove the interneuron more persistently than the depressing input synapse. These two types of spike output pattern were then used to drive different types of output synapses. The depressing output synapse was the same as in Fig. 3.7 and the facilitating output synapse was simulated by lowering the initial release probability of the BC \rightarrow PC synapse by 10 times. The

3.3 Interactions of STP in the FFI circuit

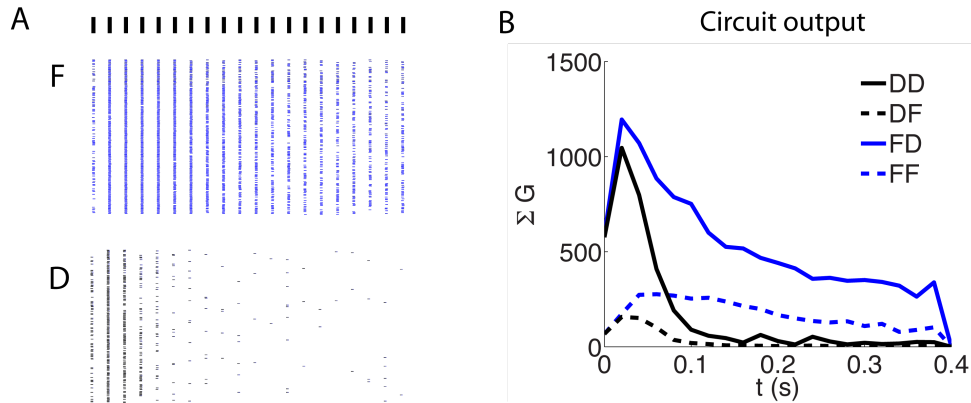


Figure 3.8: Simulation of FFI circuit with different combinations of dynamics synapses - (A) 50 Hz regular spike inputs were used to drive a facilitating (“F”) or a depressing (“D”) synapse in connection with a LIF neuron. 361 repetitions were conducted and the resulted spike outputs are shown as raster plots. The initial spiking probability in the two cases were similar. (B) The spike output from the two neurons were then fed into different dynamic synapses. The facilitating output synapse has 10 times smaller release probability than the depressing output synapse. The peak synaptic conductances were summed across 361 repetitions upon each input spike in the 50 Hz regular train. “DD ”indicates a depressing input synapse in connection with a depressing output synapse, and et al.

summed output synaptic conductances were plotted against time in Fig. 3.8B. When the input synapse was depressing, no matter how was the output synapse, the circuit output had only phasic response to the train stimulation (black curves in Fig. 3.8B). This results implied that the input depressing synapse dominated the dynamics of the circuit output and the output synaptic dynamics had little influence on the temporal structure of the circuit output. On the contrary, the facilitating input synapse could not determine the overall circuit output dynamics alone, as shown in Fig. 3.8B (blue curves). When the output synapse was also facilitating, the circuit output was kept at a constant level, meaning the circuit was generating tonic output. When the output synapse was depressing, like the case in Fig. 3.7B, the total output of the circuit was a balance between input and output synaptic dynamics. The steady-state level of the circuit output depended on the magnitude of the facilitation and depression.

3. RESULTS

3.3.2 Spike output dynamics of interneurons are regulated by input synaptic dynamics

The computer simulation has shown that the spike output of interneurons are regulated by their input synaptic dynamics. To measure the spike output of the interneurons in the real circuits, 50 Hz GC stimulation was applied and the membrane potential was recorded from BCs and SCs. The experiment was performed without SR 95531 to reveal firing patterns under physiological condition. Spiking events were plotted as a raster plot and the probability of spiking was calculated by taking the ratio between the number of evoked spikes across all the sweeps for each stimulation in the train and the total number of repeated sweeps (Fig. 3.9A, one example from each cell type). For BCs, the spiking probability decreased after the onset of the stimulation. The average spiking probability at the onset of the stimulation was $88\% \pm 4.4\%$ and it decreased to $50\% \pm 1.5\%$ 200 ms after the onset of the stimulation. GCs are known to fire at high frequency, up to hundreds of Hz under physiological condition (Chadderton et al., 2004; Jorntell and Ekerot, 2006). A high-frequency spike input from GCs would be converted to the transient spike outputs of BCs. In contrast to BC, SC had a much lower initial spiking probability which was $48\% \pm 7.7\%$ on average. The probability increased to $77\% \pm 5.5\%$ (it was significantly different comparing with the initial spiking probability, $p < 0.01$) at the third response and stayed at this level within 400 ms. Therefore, during prolonged activities in the circuit, spike outputs of SCs are more persistent than those of BCs. The initial spiking probability of interneurons reflects their input synaptic strength and their spike output dynamics are consistent with the parallel fiber synaptic dynamics. The intrinsic firing property did not further modify the interneuron spike output dynamics, which is due to the high dynamic range of spike generation from both interneurons (Fig. 3.3B).

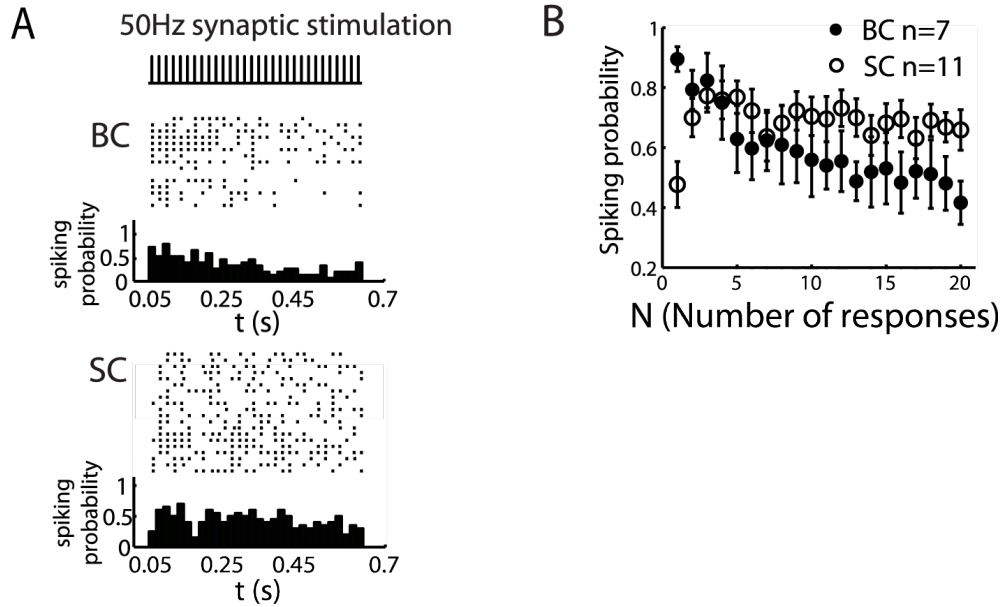


Figure 3.9: Interneuron spike output dynamics follow its input synaptic dynamics. - (A) Spikes were detected from BC and SC, and plotted as a raster plot upon a 50 Hz train of granule cell stimulation. Spikes were counted from a 5 ms time window after each stimulation pulse. Spiking probabilities are plotted beneath the raster plot. (B) Summarized spiking probability is shown for both cell types.

3.3.3 Facilitating synapses connected to depressing synapses

Dendritic FFI is mediated through a facilitating excitatory synapse and a depressing inhibitory synapse. As predicted by the simulation, the output dynamics of the dendritic FFI circuit is a balance between the facilitating excitatory synapse and the depressing inhibitory synapse. Less depressed dendritic inhibition compared with monosynaptic inhibitory output from SCs, or even tonic inhibition can be expected from the dendritic FFI circuit output. To test this experimentally, we applied spike patterns obtained in Fig. 3.9 (the spike pattern of one example stellate cell recorded by stimulating GCs) into a single stellate cell and examined the resulting IPSCs recorded from the PC which was innervated by the SC. The PC was voltage-clamped with a patch pipette containing Cesium and high $[Cl^-]$. Fig. 3.10 shows the average IPSCs obtained from “realistic” spike patterns. In contrast to a regular spike train (Fig. 3.6), the average IPSCs showed facilitation. The data are summarized from 7 cells in Fig. 3.10B, which shows persistent

3. RESULTS

inhibitory input to PC under this stimulation protocol.

A high failure rate of spiking from SC can be observed from Fig. 3.9 and especially the initial firing probability is small comparing with BC. This correlates with the input synaptic dynamics of the interneurons. GC \rightarrow SC synapse is facilitating, so most likely the initial release probability at this synapse is low and the synaptic transmission is unreliable. But under high frequency spikes input, the synaptic strength is enhanced and the synapse becomes more reliable (Fig. 3.9B). Because of the small size of the GC synapse and the stochastic nature of the synaptic transmission, stellate cells do not fire each time when an excitatory input comes even with the enhanced synaptic strength. This further relieves the depression of SC's output synapse. It is likely that both facilitating input synapse and the high failure rate of spike output of the SC balance the depressing output synapse of the SC for maintaining a persistent circuit output. As shown in Fig 3.9, failure rates of spiking in response to granule cells stimulation varied among cells. The experiment in Fig. 3.10 applied an example stellate cell firing pattern with a small initial firing probability. Therefore, it is possible that the dendritic FFI circuit output shows less facilitation when the initial firing probabilities are higher at the stellate cells, and as a result, overall dendritic inhibition from multiple SCs is less facilitative than the one seen in Fig 3.10.

The "realistic" SC spike pattern experiment has demonstrated the persistent inhibitory output from a dendritic FFI circuit despite of the depressing stellate cell synapse. Next, in order to examine whether a Purkinje cell receives persistent inhibition at the dendrite, I performed dendritic patch clamp recordings to isolate dendritic inhibition from somatic inhibition. Dendritic patch clamp was performed on the dendritic arbor of a PC, more than 100 μm from the soma (Fig. 3.11A). A 50 Hz GC stimulation protocol was the same as in Fig. 3.4. Dendritic membrane potentials were recorded from the dendritic patch pipette shown as the black trace in Fig. 3.11B (top panel). When the inhibitory synaptic inputs were blocked by SR 95531, I recorded the excitatory post-synaptic potentials (EPSPs) shown as the gray trace under the same stimulation condition as control. Each

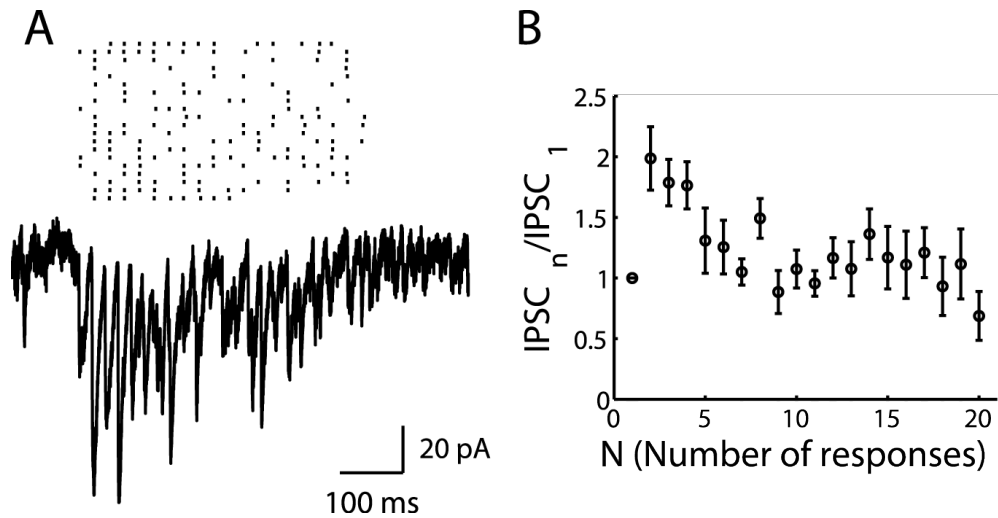


Figure 3.10: Inhibitory output driven by realistic firing pattern of SC under 50 Hz GC stimulation - (A) Firing patterns of an example SC in response to the GC stimulation at 50 Hz (Fig. 3.9) was applied to stellate cells. 20 different patterns were applied, and the resulting IPSCs from the PC were averaged (bottom trace). (B) The summary of normalized peak amplitudes from 7 cells.

trace is an average of 5 sweeps. GC stimulation pipette was placed on the side of the recording dendritic branch and the intensity was adjusted to the minimum in order to minimize the recruitment of somatic activation. In the presence of inhibition, the dendritic depolarization during the train was limited. The decay of each response was also accelerated. To show this more clearly, each individual PSP in the train was offset by the decay of its previous response (Fig. 3.11B, bottom panel) in order to retrieve the evolution of membrane potential due to the slow decay of synaptic current. Contribution of inhibitory postsynaptic potentials (IPSPs) was then calculated by subtracting the two traces (Fig. 3.11C). The normalized peak amplitudes of IPSPs were plotted in Fig. 3.11D (an average from 3 cells), showing a slight depression ($80\% \pm 4.7\%$ steady state depression averaged from the last 10 responses). Compared with the direct stimulation of an SC at 50 Hz in Fig. 3.6 ($42\% \pm 1.9\%$ steady state depression), inhibition depressed much less when GCs were stimulated. In the experiment of Fig. 3.11, inhibitory conductance was not directly measured because of the difficulty of dendritic voltage clamp. Using current clamp does not necessarily measure the inhibitory synaptic conductance due to confounding effects such as activation of

3. RESULTS

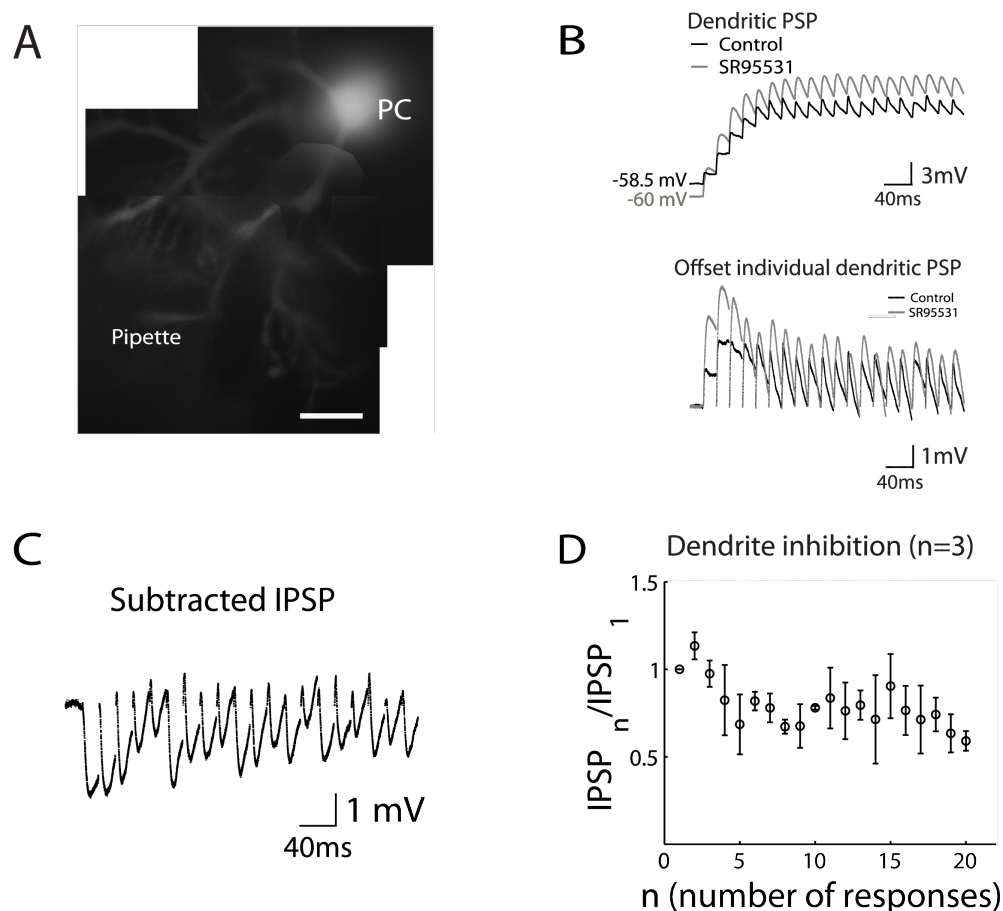


Figure 3.11: Dendritic feed-forward inhibition recording - (A) Superimposed images show a PC soma with part of its dendrite. Alexa 488 was loaded from the soma and the position of the "Pipette" indicates the recording site on the dendrite. The scale bar is 20 μm . (B) Postsynaptic potentials (PSPs) were recorded from the dendritic patch pipette upon a 50 Hz granule cell stimulation in both control (black) and the presence of SR 95531 (gray) condition (top panel). Each PSP was offset by the decay of its previous response to highlight the difference between the two conditions upon each stimulation during the train (bottom panel). (C) Subtracting the two traces in (B, bottom panel) resulted in IPSPs which were blocked by SR 95531. (D) The peak value of each IPSP during the train was normalized to the first one. An average of 3 cells is plotted against the number of responses showing $80\% \pm 4.7\%$ steady state depression. Resting membrane potential at the dendrite was -60.5 ± 1.5 mV (control) and -64.2 ± 2.1 mV (SR 95531). Resting membrane potential at the soma was -59.5 ± 0.7 mV (control) and -62.3 ± 2.4 mV (SR 95531)

3.3 Interactions of STP in the FFI circuit

voltage gated channels and changes in the driving force of channels. Since voltage changes were relatively small in our experiments, the above issues are not serious. Together with Fig. 3.10, it is likely that the total dendritic inhibition is recruited persistently under high-frequency GC inputs ($50 \text{ Hz} \times 20$) as a result of the counter-balance between the facilitating excitatory and depressing inhibitory synapse. Note that other factors also contribute to persistent inhibition: most likely, multiple SCs contribute to dendritic inhibitions and SCs do not always fire in response to the GC stimulation (Fig. 3.9, 3.10). Combination of these two factors may further counteract with depression of SC \rightarrow PC synapses. Compared with Fig. 3.10, dendritic inhibition is less facilitative in Fig. 3.11. This is because the initial spiking probabilities are variable among stellate cells and some FFI circuits have less output facilitation or even slight depression when the initial spiking probability is high. As a result, overall dendritic inhibition may become less facilitative.

3.3.4 Two depressing synapses in series

Both the input and output synapses are depressing for basket cells. A depressing synapse responds only to the transient input. As predicted by the model circuit, the output from two depressing synapses in a row has only phasic response to the 50 Hz input spike train. To demonstrate this experimentally, I performed simultaneous patch clamp recordings on a pair of connected BC and PC as in Fig. 3.12 under 50 Hz trains of GCs stimulation. When the BC was in current clamp mode (control condition), it fired when the excitatory inputs from GCs exceeded the spiking threshold. The synaptic current recorded from the PC is shown as a black trace in Fig. 3.12. It consists of monosynaptic excitatory currents and feed-forward inhibitory currents (as in Fig. 3.4). When the BC was voltage clamped at -70 mV to prevent firing, we considered this BC to be silenced (gray in Fig. 3.12). Each trace is an average of 10-20 sweeps in the two conditions. Subtraction of these two traces resulted in the inhibitory current from the recorded basket cell to the Purkinje cell through the FFI circuit, which showed substantial depression

3. RESULTS

within tens of milliseconds. An average of $40\% \pm 5.8\%$ steady-state depression was estimated from 4 cells.

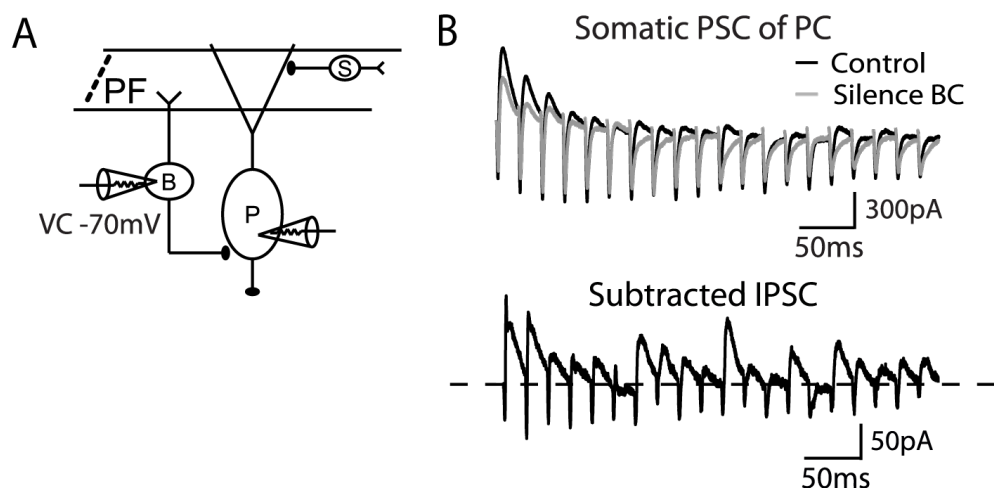


Figure 3.12: Silencing a single basket cell indicates phasic somatic inhibition. - (A) A diagram showing the experimental scheme of silencing one BC by voltage clamping the BC at -70 mV during a paired recording of BC and PC. (B) Somatic PSCs recorded from the PC under 50 Hz GC stimulations are shown in control condition (black, when the BC is under current clamp mode) and in the condition when the BC is silenced (gray). Subtracting the two traces shows the IPSCs delivered by one BC onto the soma of the PC (bottom panel). Zero level is indicated as a dotted line. An average of $40\% \pm 5.8\%$ steady state depression was observed from 4 cells.

Somatic inhibition of Purkinje cell is mediated by large basket cell inputs. The IPSCs measured from a PC soma in response to GCs stimulation are the summation of somatic and dendritic inhibition from populations of BCs and SCs, which can be estimated by subtracting the synaptic currents with and without SR 95531 (Fig. 3.13A). We observed that IPSCs were depressed to $48\% \pm 1.5\%$ during 50 Hz GC stimulation (Fig. 3.13B). Since dendritic inhibition did not show such strong depression (Fig. 3.10, 3.11), the depression of di-synaptic IPSCs seen in Fig. 3.13 must be determined by the GC \rightarrow BC \rightarrow PC pathway. The steady-state of single BC di-synaptic inhibition (Fig. 3.12) was close to the macroscopic di-synaptic IPSCs (Table 3.1), suggesting that a majority of somatic IPSCs were contributed by basket cells. These two experiments proved that phasic somatic

3.3 Interactions of STP in the FFI circuit

inhibition which was first presented in Fig. 3.4 is a consequence of $GC \rightarrow BC$ and $BC \rightarrow PC$ synapses in series, both of which are depressing.

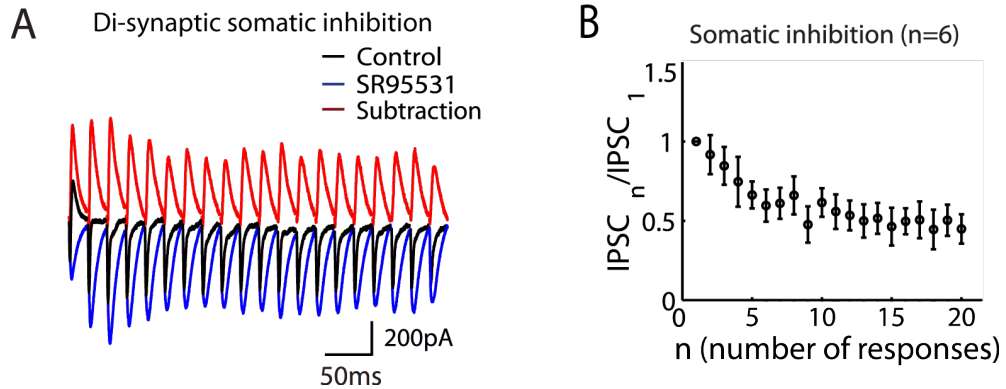


Figure 3.13: Phasic somatic inhibition - (A) Somatic recorded PSCs from a PC under 50 Hz GC stimulations are shown in both control (black) and SR 95531 (blue) condition. Subtracting the two traces gave an estimation of somatic IPSCs (red). (B) Normalized IPSCs were averaged from 6 cells showing $48\% \pm 1.5\%$ steady state depression.

Table 3.1: The steady-state level of inhibition

steady-state inhibition	SC	BC
monosynaptic ⁽¹⁾	$42\% \pm 1.9\%$	$43\% \pm 1.5\%$
di-synaptic ⁽²⁾	$108\% \pm 5.8\%$	$40\% \pm 5.8\%$
macroscopic ⁽³⁾	$80\% \pm 4.7\%$	$48\% \pm 1.5\%$

(1) Direct stimulation of MLIs at 50 Hz

(2) A single MLI output to a Purkinje cell upon 50 Hz GCs stimulation

(3) Dendritic or somatic recording from PC under 50 Hz GCs stimulation which recruit populations of MLIs

3. RESULTS

3.4 Change of synaptic dynamics alters circuit dynamics

Through comparison between somatic and dendritic FFI circuit which differed only at the dynamics of one synapse, it was demonstrated that the dynamics of the circuit output depended on the synaptic dynamics. To further reveal the functional consequence of short-term synaptic plasticity in regulating the circuit dynamics, I applied two methods to change the short-term plasticity of a synapse in the circuit and observed the consequence on the circuit output. One method is to interfere with the molecular mechanism which underlies the synaptic transmission and plasticity. The other method is to create an artificial synapse with desired short-term dynamics in the circuit.

3.4.1 Munc13-3 knockout mice turns depressing synapses to facilitating synapses

One mechanism underlying short-term synaptic plasticity is the release probability. Synapses with higher release probability tend to show depression and if the release probability is lowered by reducing the influx of Ca^{2+} , facilitation can be observed from some synapses (Wright et al., 1996; Kreitzer and Regehr, 2000). The short-term plasticity of a synapse can be changed if the release probability is altered. Target-dependent synaptic plasticity is known to be mainly mediated by presynaptic mechanisms such as differences in release probability among synapses (Beierlein et al., 2007; Reyes et al., 1998; Lawrence and McBain, 2003). Munc13-3 is a cerebellar-specific isoform from the presynaptic protein Munc13 family which is implicated in working on synaptic vesicle priming (Augustin et al., 1999; Augustin et al., 2001; Basu et al., 2007). Deletion of Munc13-3 has been shown to induce an increase of the paired-pulse facilitation in granule cell \rightarrow Golgi cell synapses (Beierlein et al., 2007) through lowering the release probability. I observed an increase of the paired-pulse facilitation also in GC \rightarrow BC synapse (Fig. 3.14), while no significant changes in GC \rightarrow PC and GC \rightarrow SC synapses. Inhibitory synapses were not affected by deletion of Munc13-3. For FFI circuit, GC

3.4 Change of synaptic dynamics alters circuit dynamics

→ BC synapses on the somatic pathway behaves similar as GC → SC synapses on the dendritic pathway in Munc13-3 knockout mice.

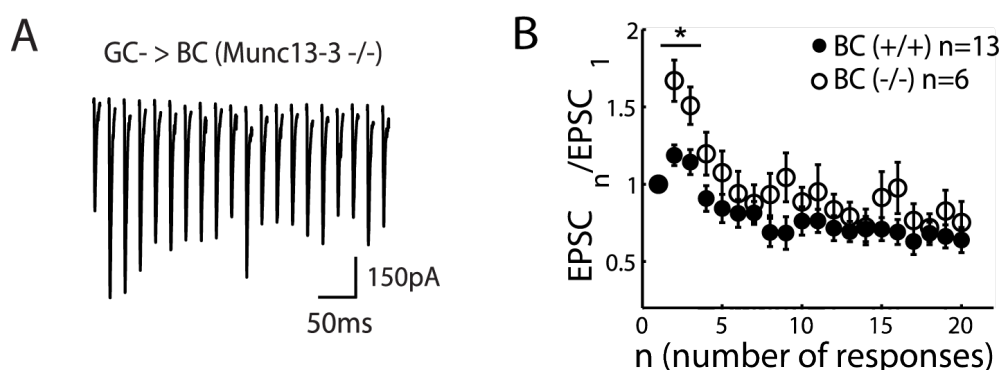


Figure 3.14: Deletion of Munc13-3 enhances the paired-pulse facilitation at GC → BC synapse. - (A) An example trace of EPSCs recorded from a basket cell of Munc13-3 KO mice shows no depression. The cell was voltage clamped at -65 mV in the presence of SR 95531 and 50 Hz trains of stimulation were applied to the granule cell layer. (B) Normalized EPSCs were averaged from 6 recordings in KO mice (open circles) presenting a significant increase of the paired-pulse ratio comparing with their wild type litter mates (filled circles). (* indicates $p < 0.01$)

Since the dynamics of GC → BC synapses are modified in Munc13-3 knockout mice, one would expect that the output of somatic FFI circuit will be affected and behaves like the dendritic FFI circuit. Indeed, as shown in Fig. 3.15, somatic di-synaptic IPSCs showed facilitation lasting more than 100 ms after the onset of 50 Hz stimulation in KO mice (significant facilitation comparing with wildtype mice, $p < 0.05$). The steady-state was also less depressed ($61.7\% \pm 1.7\%$) than that measured from the wildtype animals (Table 3.1). It is important to note that the synaptic connections other than GC → BC synapse are unchanged in Munc13-3 KO mice.

3. RESULTS

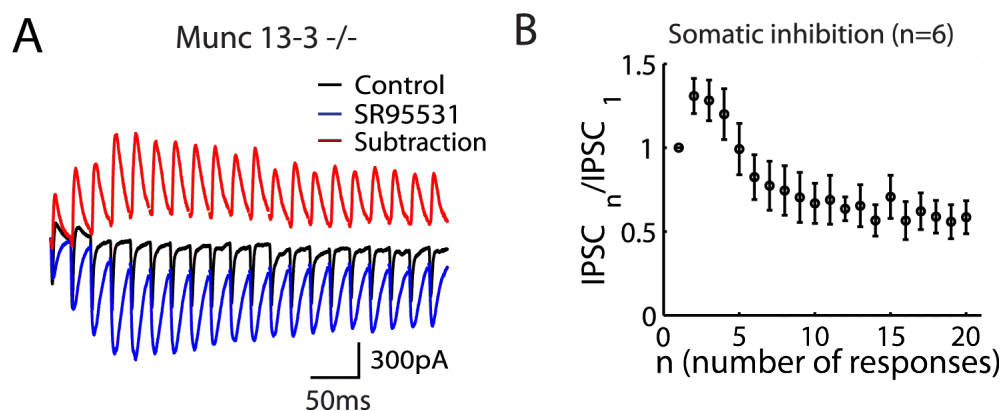


Figure 3.15: Somatic feed-forward inhibition is more facilitating in Munc13-3 knockout mice. - (A) Somatic recorded PSCs of a Purkinje cell from a Munc13-3 KO mouse under 50 Hz GC stimulations are shown in both control (black) and SR 95531 (blue) condition. Subtracting the two traces gave an estimation of somatic IPSCs (red). (B) Normalized IPSCs were averaged from 6 cells.

3.4.2 Simulating artificial synaptic dynamics with dynamic clamp

Dynamic clamp technique enables computer simulation directly on the real neuronal circuit (Prinz et al., 2004). Artificial conductances can be injected to the neuron which is under patch clamp recording, and the consequence of the injected conductances can be observed almost simultaneously. To alter synaptic dynamics in the neuronal circuit, a phenomenological synaptic dynamics model (Tsodyks and Markram, 1997) is chosen for simulating the desired synaptic dynamics. Basket cells have depressing inhibitory output synapses to Purkinje cell soma and the release probability is estimated from the same model as ~ 0.2 . When stimulating GCs as the input to the FFI circuit, the spike output of a Purkinje cell was recorded under the current clamp mode. The spikes were plotted as a raster plot in Fig. 3.16. In the control condition, no interference was introduced to the slice and the observed spike pattern from the PC indicated that the responsiveness of the PC increased during the 50 Hz train of stimulation (Fig. 3.16A, top panel). This is due to the depressed feed-forward inhibitory input to the PC, as we have observed no change of the PC responsiveness when the inhibition was blocked by SR 95531 (Fig. 3.16A, bottom panel). From Fig. 3.16A one can

3.4 Change of synaptic dynamics alters circuit dynamics

observe the function of feed-forward inhibition as shunting the PC rapidly after each GC spike input, which leaves a very small time window for the integration of excitatory inputs. Therefore at the onset of the 50 Hz train, only single spike outputs from the PC were observed; and from the 3rd to 4th stimulation, double spikes appear due to the broadening of the synaptic integration time window.

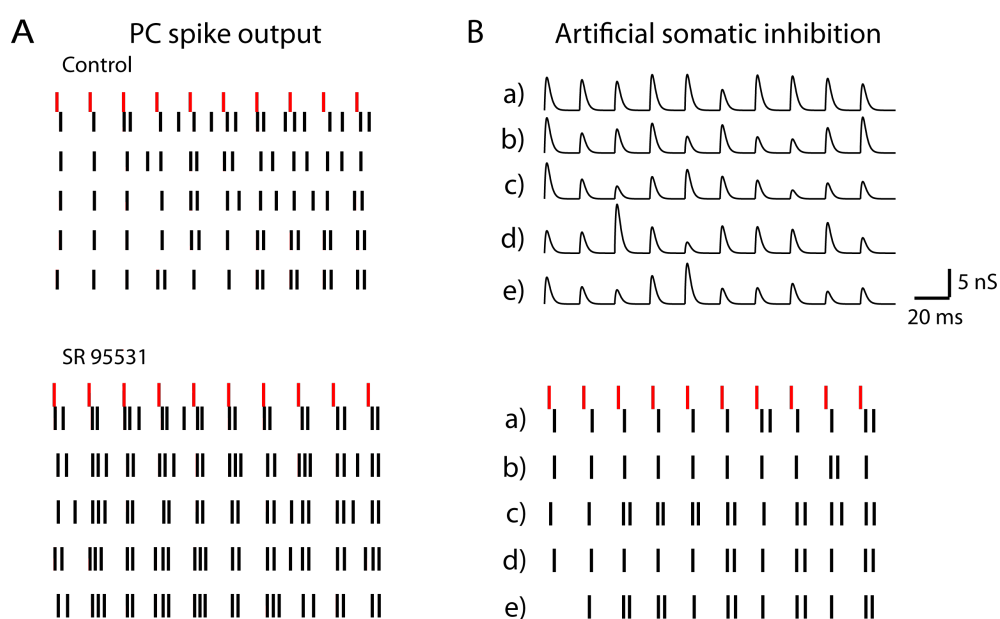


Figure 3.16: Spike output of Purkinje cell - (A) Raster plots of PC spikes under 50 Hz GC stimulation. Top panel (control condition): the GC stimulation is indicated by the red plot and the resulted PC spikes are shown for 5 repetitions. Bottom panel shows the similar recording when SR 95531 was perfused to the slice. (B) Artificial inhibitory conductances were injected to the PC soma through dynamic clamp. 5 conductance traces are the simulated stochastic dynamic conductance from a phenomenological model (Tsodyks and Markram, 1997) (top panel). In the simulation, the release probability was lowered 10 times than the actual release probability from the fit to the IPSCs of BC \rightarrow PC synapses. All the real inhibitory inputs were blocked by SR 95531 in this experiment and the resulted PC spike output is shown in the bottom panel.

In the control condition, the feedforward inhibition arrives only at the onset of the stimulation and if the FFI comes more persistently, one would expect to see less double spikes during the train. To demonstrate this, under the condition that the

3. RESULTS

natural inhibitory input was blocked by SR 95531 in the brain slice, the artificial inhibitory conductance was injected to the soma of the PC with 3 ms delay to the onset of each GCs stimulation. Single depletion model (Eq. 1.11) was simulated to generate synaptic conductances with 10 times lowered release probability than the real BC \rightarrow PC synapse. The recovery time constant τ_r was also increased to 100 ms. Stochastic simulations were run by the computer of the dynamic clamp with the algorithm described in Sec. 2.6.2. 5 traces of the dynamic conductances were shown in Fig. 3.16B (top panel), and due to the stochasticity the dynamics differ between each trace. Trace a), b) and d) have less depression compared with c) and e). The resulted PC spike output sequences (Fig. 3.16B, bottom panel) have less double spikes in a), b) and d) when the inhibitory synaptic conductances are more persistent, while more double spikes appear in c) and e) when the conductances are more depressed. The correlation between the dynamics of the synaptic conductance and the output pattern of the PC can be observed from Fig. 3.16, but more trials of experiments are necessary to obtain a quantitative results.

4

Discussion

The nervous system operates dynamically to allow animals to adapt to the changing environments. During ongoing activities various forms of plasticity occur at all levels of the nervous system, from single ion channels to synaptic connections and neuronal circuits. To understand the consequence of the plasticity at each level and how the various forms of plasticity concert to generate behavior is an important key to understand neuronal machinery. Both theoretical and experimental work are needed to find out the algorithms of the plasticity. The theoretical approach can predict the dynamics of a large neuronal circuit with its building blocks, like synapses and spiking neurons, which compensates the limitation of the experimental work due to the difficulty of manipulating certain variables in a real neuronal system. At the same time, the experimental work is essential for characterizing accurately the behavior of each building block and testing the prediction from a theory. The major contribution of this work is that the dependence of the circuit dynamics on the synaptic dynamics has been characterized experimentally by comparing two circuits which differ only at one synapse. Besides, the experiments also demonstrated that artificial alterations to the synaptic dynamics led to the change in the circuit dynamics. It remains several issues to be further studied, like the interaction between the synaptic dynamics and the intrinsic firing properties of individual neurons, the mechanisms underlying synaptic plasticity and the functional relevance of the circuit dynamics. They will be discussed in more details in this section.

4.1 The determinants of neuronal circuit dynamics

Excitatory and inhibitory neurons interconnected with dynamic synapses can form a large number of microcircuits, which could resemble the construction of electronic circuits by resistors, capacitors, transistors and so on. The dynamics of different neuronal microcircuits depends on the connectivity pattern of neurons and physiological properties of the various synaptic pathways. Neural microcircuits across various species and brain regions varies in terms of the type of neurons, neurotransmitters, synaptic kinetics, short-term and long-term synaptic plasticity. Moreover, they can be very different in terms of the precise connectivity and the input - output relationship which render different circuits to achieve specific functions. The first step to characterize a circuit is to find out its input-output relationship and the dynamics of the relationship. Once the dynamics of the circuit is fully described in terms of the parameters of its building blocks (neurons and synapses), the functions which this circuit performs can be easily deduced and the consequence of changing the circuit parameters can be predicted.

Feed-forward inhibitory circuit is one of the simplest neuronal circuit and it exists in lots of functional circuits in different brain areas (Callaway, 2004; Swadlow, 2003; Blitz and Regehr, 2005; D'Angelo and Zeeuw, 2009). A FFI circuit is constructed with three building blocks: an input synapse, an interneuron, and an output synapse. How the circuit dynamics depends on the connecting synaptic dynamics has been investigated from both computational and experimental approaches here. The output dynamics of cerebellar FFI circuits are mainly determined by the connecting synapses because the interneurons, both the basket cell and the stellate cell, in the cerebellar FFI circuit are fast spiking neurons with a large dynamic range for spike generation. They both can fire up to 400 Hz regular spikes under constant current injection without adaptation. This property makes the output firing rate of the neuron follows linearly the input strength within the dynamic range of the interneuron spike generation. If the intrinsic firing property of the interneuron is different from that of the fast spiking neuron and spike output does not linearly depend on the input synaptic strength, the

4.2 Mechanisms of target-dependent synaptic plasticity

circuit dynamics will depend not only on the synapse but also on the intrinsic neuronal processing. It was demonstrated in this work that the input excitatory synaptic dynamics was the major determinant of the overall circuit dynamics in the cerebellar FFI circuits, while at the same time various forms of neuronal modulation have been discovered in the cerebellar cortex (Diana et al., 2002; Stell et al., 2007) which will contribute to the modification of the circuit output depending on the specific activity pattern through interfering with the synaptic parameters.

4.2 Mechanisms of target-dependent synaptic plasticity

The granule cell synapses present target-dependent plasticity, a phenomenon which has been identified also in other systems (Katz et al., 1993; Rosenmund et al., 1993; Scanziani et al., 1998; Reyes et al., 1998; Lawrence and McBain, 2003). In cerebellum, the granule cell synapse has always been considered as a facilitating synapse (Konnerth et al., 1990; Dittman et al., 2000; Beierlein et al., 2007), while it has been reported that the amplitude of facilitation differs depending on the target neurons and the way of stimulation (Isope and Barbour, 2002; Sims and Hartell, 2006; Beierlein et al., 2007). Unexpectedly, this is not the case for GC \rightarrow BC synapses, which exhibit synaptic depression. The difference between the facilitating and depressing GC synapses may arise from the development. To test this possibility, the paired-pulse ratio which differed significantly between facilitating and depressing synapses was plotted against the postnatal age of the animals which were used for the entire work. Fig. 4.1 shows the results from three GC target cell groups. No significant age dependence was observed from all the cell groups, which indicated that the target-dependent plasticity did not depend on the age within the tested range.

4. DISCUSSION

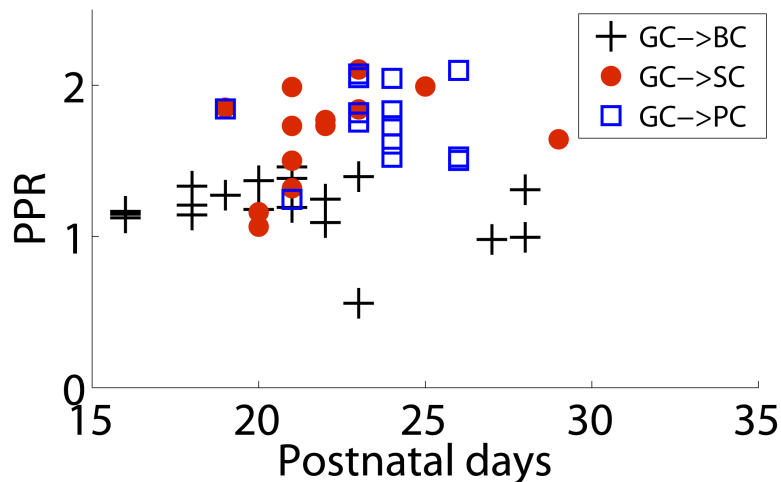


Figure 4.1: The age dependence of the granule cell synaptic plasticity - Paired-pulse ratios ($EPSC_2/EPSC_1$) of GC synapse onto three post-synaptic targets under 50 Hz granule cell stimulation are plotted against postnatal days of the animals. Data were recorded when inhibitory inputs were blocked.

The different synaptic plasticity can result from the different synaptic locations on the granule cell axon (Sims and Hartell, 2005). Stellate cells locate at more distal areas to the granule cell layer than basket cells, therefore stellate cells are more innervated by the parallel fiber synapses while basket cells are innervated by both the parallel fiber synapses and the ascending axon synapses. In the experiments, depending on the location of the stimulation electrode, one can selectively recruit the ascending axon synapses or parallel fiber synapses in cerebellum. I have not observed any dependence of the short-term synaptic plasticity on the location of the stimulation electrode in the granule cell layer, which implies that the synaptic location is not the major origin of the differential synaptic plasticity.

Target-dependent synaptic plasticity is known to be mainly mediated by presynaptic mechanisms such as differences in release probability among synapses (Reyes et al., 1998; Lawrence and McBain, 2003; Beierlein et al., 2007). The postsynaptic mechanisms such as receptor desensitization (Jones and Westbrook, 1996; Trussell and Fischbach, 1989) and saturation (Tong and Jahr, 1994) could

4.2 Mechanisms of target-dependent synaptic plasticity

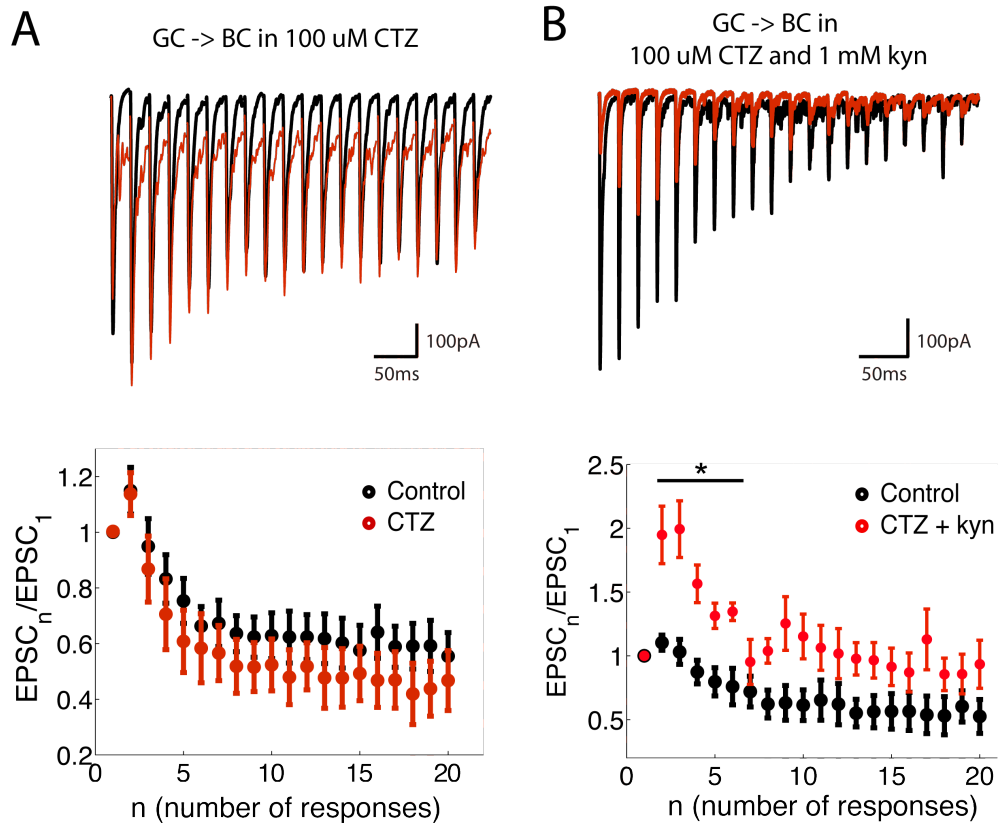


Figure 4.2: Postsynaptic receptor saturation is the underlying mechanism for the depressing synapse. - (A) Postsynaptic responses from BC during 50 Hz GC stimulations under control (black) and 100 μ M CTZ (red) in the presence of SR 95531. CTZ did not alter the synaptic depression time course for GC \rightarrow BC synapses. Normalized EPSCs summarized from 6 cells is shown in the bottom panel. Note that no significant difference is observed between the two conditions, indicating desensitization of AMPA receptors is not responsible for synaptic depression, unlike a large synapse in the auditory pathways (Trussell and Fischbach, 1989). (B) When 1 mM Kyn was also added to the extracellular solution, the amplitudes of EPSCs recorded from BCs were decreased and the time course of depression was changed. Other experiment condition is the same as in (A). Normalized EPSCs are plotted against the number of responses in comparison between normal Ringer solution and CTZ+kyn solution (bottom panel). Significant difference was observed from the 2nd to 6th response ($n=5$ cells, * indicates $p < 0.001$). Steady-state level was above the control, although they were not significant different.

play roles as well. I first examined whether postsynaptic receptor desensitization was responsible for target-dependent plasticity of granule cell synapses. When I

4. DISCUSSION

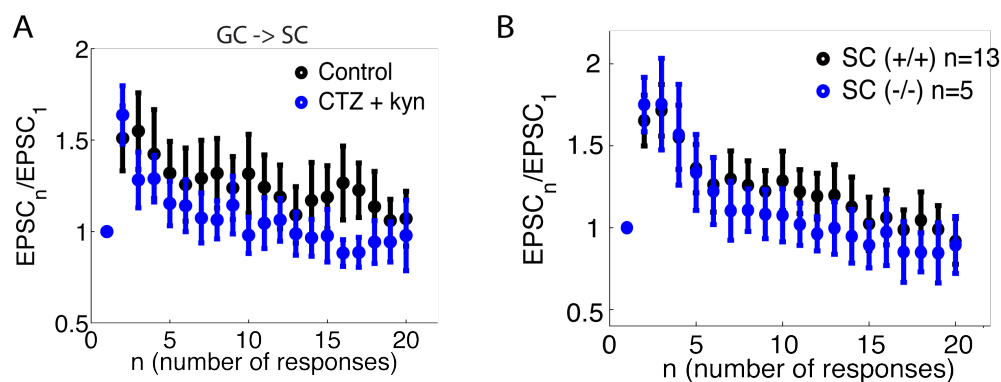


Figure 4.3: Removal of receptor saturation and Munc13-3 deletion do not change the facilitation at GC \rightarrow SC synapse. - (A) Normalized EPSCs recorded from SCs inringer solution (Control) were compare with recordings from SCs in extracellular solution containing 100 μ M CTZ and 1 mM Kyn under 50 Hz GCs stimulation (n=6 cells). No significant difference was observed. Inhibitory inputs were blocked by SR 95531 during the experiments. (B) Normalized EPSCs recorded from SCs of Munc13-3 wildtype mice were compare with recordings from SCs of knockout mice under 50 Hz GCs stimulation. No significant difference was observed. Inhibitory inputs were blocked by SR 95531 during the experiments.

applied cyclothiazide (CTZ, 100 μ M), a blocker of AMPA receptor desensitization, the time course of synaptic depression at GC \rightarrow BC synapse was unchanged (Fig. 4.2A) indicating no role of postsynaptic receptor desensitization in the synaptic depression. Then, I applied kynurenic acid (Kyn, 1 mM), a low affinity competitive antagonist of AMPA receptors, in addition to CTZ, to examine whether postsynaptic receptor saturation played a role. GC \rightarrow BC synapses behaved like GC \rightarrow SC synapses after removing the receptor saturation (Fig. 4.2B). An average from 5 cells showed significant increase of facilitation lasting about 100 ms after the onset of the stimulation. On the other hand, the short-term plasticity of GC \rightarrow SC synapses had little change after application of CTZ + Kyn (Fig. 4.3A). To account for the change in the time course of short-term plasticity by CTZ + kyn, one has to postulate multivesicular (MV) release (Tong and Jahr, 1994) at GC \rightarrow BC synapses in addition to receptor saturation (Fig. 4.4A), since the amplitude of glutamate concentration must have changed during repetitive stimulations. This is because kyn would not change the time course

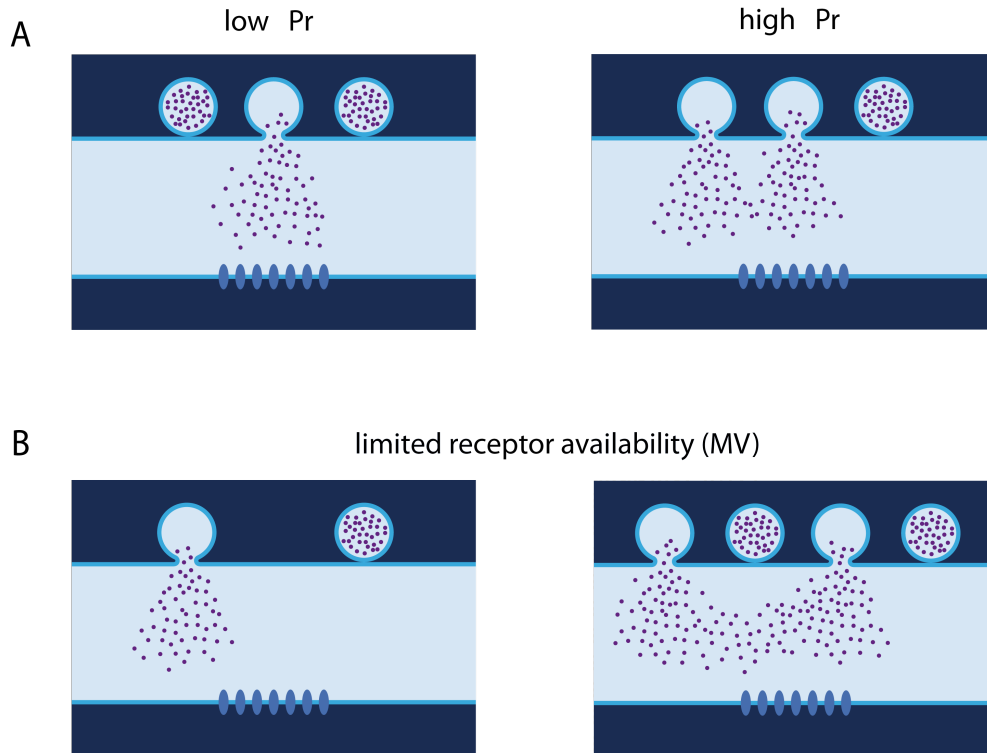


Figure 4.4: Multivesicular release and postsynaptic receptor saturation work synergistically to cause the synaptic depression in GC → BC synapses. - (A) The scheme shows what is happening at GC → BC synapse during repetitive stimulation. When the release probability of a release site is low, single vesicle is released and the quanta content of a vesicle is enough to occupy almost all the available postsynaptic receptors. When release probability is increased due to the ongoing activity, multiple vesicles will be released and the postsynaptic receptors are saturated by the increased glutamate concentration in the synaptic cleft. The synapse exhibits no facilitation unless the saturation is removed. (B) The deletion of Munc13-3 may result in the decreased number of primed vesicles at each release site (left) while the release probability is not changed compared with the case in wild type (right). Multivesicular release and the receptor saturation do not happen at Munc13-3 knockout mice. Therefore GC → BC synapses show facilitation in Munc13-3 KO mice.

of plasticity if only single vesicle is released per release site upon an AP: the amplitude of glutamate transient stays the same in this case and kyn scales down the response only linearly. Therefore, both pre- (multivesicular release) and post-synaptic factors (receptor saturation) are responsible for the depressing feature of PF synapses when the postsynaptic target is a basket cell. We further spec-

4. DISCUSSION

ulate that unlike the target-dependent synaptic plasticity in other synapses, the vesicular release probability is probably similar between GC \rightarrow BC and GC \rightarrow SC synapses, because the time course of facilitation during an AP train is similar under CTZ + Kyn condition. Under control condition, when the release probability is enhanced during the repetitive input, the multivesicular release happens at GC \rightarrow BC synapse and the receptor saturation prevents us from observing the facilitation nature of this synapse.

To account for the receptor saturation, one has to postulate that multivesicular release happens more frequently (or more primed vesicles exist per release site) at GC \rightarrow BC synapse because the amplitude of glutamate concentration changes only in the case of multivesicular release (Tong and Jahr, 1994). This does not exclude the possibility that multivesicular release takes place also at GC \rightarrow SC synapse (Bender et al., 2009). However receptors were not saturated at GC \rightarrow SC synapses because the time course of synaptic facilitation was not changed in the presence of CTZ + Kyn.

In Fig. 3.14, we showed an increase of the paired-pulse ratio in GC \rightarrow BC synapses of Munc13-3 knockout mice. No change of synaptic plasticity was observed from GC \rightarrow SC synapses (Fig. 4.3B). The deletion of Munc13-3 makes the GC \rightarrow BC synapses more facilitating like GC \rightarrow SC synapses, which implies that receptor saturation is relieved in Munc13-3 knockout mice. Therefore we suggest that the results of Munc13-3 KO mice may be explained in the context of multivesicular release and receptor saturation. As the first possibility, the geometrical arrangement of AMPA receptors may differ depending on the expression of Munc13-3, because Munc13-3 is a part of active zone protein complex that is linked to the postsynaptic protein scaffold. However, there is no direct evidence supporting such a role of Munc13. Secondly, Munc13-3 may regulate the number of available synaptic vesicles per release site by increasing the rates of synaptic vesicle priming. This results in more primed synaptic vesicles per release site without altering vesicular release probability (Fig. 4.4B). This is a more likely scenario because Munc13 is known to mediate synaptic vesicle priming (Rosenmund et al., 2002; Basu et al., 2007). It remains to be seen if similar mechanisms can account for

4.3 Functional implications in cerebellar information processing

target-dependent synaptic plasticity in other preparations.

4.3 Functional implications in cerebellar information processing

Microcircuits are the building blocks for the whole brain machine and they use excitatory and inhibitory neurons interconnected with dynamic synapses to execute specific functions. In the cerebellum, two feed-forward inhibition circuits receive the same input and target onto different subcellular compartments of Purkinje cell, making somatic and dendritic inhibition. They have different output strengths and distinct output dynamics under the same input, which renders them to process different information and exert differential control over their targets.

Unlike neocortical (Beierlein et al., 2003) and hippocampal inhibitory circuits (Pouille and Scanziani, 2004; Hefft and Jonas, 2005) where different types of interneurons are recruited, in the cerebellar FFI circuit, both types of molecular layer interneurons are fast spiking neurons and their output synapses exhibit similar short-term dynamics. This supports the idea that BC and SC are similar types of interneurons which differ only in morphology and spatial distribution within the molecular layer (Sultan and Bower, 1998). Connections made by a BC and a SC onto the soma and dendrite of a PC have a 7-fold difference in synaptic strength. This difference is about twice as large as reported previously in the young rat (Vincent and Marty, 1996). However, it contrasts with the somatic and dendritic inhibition in the hippocampus (Miles et al., 1996) where less than a 2-fold difference in synaptic strength was reported. One parallel fiber makes one or two synapses with a PC (Palay and Chan-Palay, 1974) and unitary granule cell → Purkinje cell connection is weak (Isope and Barbour, 2002). If the main function of the dendritic FFI is to balance the excitation, a comparable inhibitory synaptic strength with excitatory one will be the optimal solution concerning both function

4. DISCUSSION

and energy consumption (Niven and Laughlin, 2008). As for somatic inhibition, it confronts strong PF inputs summed over the entire dendrites and climbing fiber inputs (Eccles et al., 1966b). A strong inhibitory synapse is recruited at the soma in order to balance strong excitatory inputs and inhibit the spike output of the Purkinje cell. This work showed both BC and SC had broad dynamic range for spike generation (the feature of fast spiking neuron). Within this range the input synaptic strength could be linearly transformed to the output firing rate. As a consequence, the dynamics of PF synapses are the main determinants for the recruitment of interneurons in the cerebellar FFI circuit. Furthermore, since BC and SC share similar output synaptic dynamics, both FFI circuit will be tightly regulated by the dynamics of excitatory inputs to the circuit, which is different from inhibitory circuits in other brain regions (Beierlein et al., 2003; Pouille and Scanziani, 2004) where various types of interneurons show distinct forms of short-term synaptic plasticity.

Inhibitory circuits are recruited in a frequency-dependent manner in both hippocampal FFI circuits (Mori et al., 2004; Klyachko and Stevens, 2006) and feedback circuits (Pouille and Scanziani, 2004). A similar phenomenon has been revealed from this study in the cerebellum, and further it was shown that the frequency-dependent recruitment depended on the targeted subcellular compartments (soma vs. dendrite). Driven by high-frequency GC inputs (Chadderton et al., 2004; Jorntell and Ekerot, 2006), the somatic FFI circuit operates more effectively at the onset of the input while the dendritic FFI circuit can follow the activity of GCs. Note that difference in the magnitude of short-term synaptic plasticity between GC to BC and SC synapses was largest in the first five or ten stimulations. Under physiological conditions, such a number of spikes were elicited by sensory stimulation (Chadderton et al., 2004). Another possible consequence of the depressing feature of the somatic inhibition is to detect synchronized activities of multiple BCs which innervate the same PC. In vivo, molecular layer interneurons fire spontaneously at low rates (Eccles et al., 1966c; Vincent and Marty, 1993; Häusser and Clark, 1997). Because of slow recovery from synaptic depression (Sakaba, 2008), each BC input may be already at the depressed state in the presence of spontaneous activities. Then, only when

4.3 Functional implications in cerebellar information processing

several BCs fire simultaneously, a substantial inhibition can inhibit the spike output of the PC. The BCs which innervate the same PC lie in the plane orthogonal to the PFs, and each PC is innervated by multiple BCs (Palay and Chan-Palay, 1974). A preliminary study implied that the synaptic strength and the dynamics between BC and PC did not vary as a function of the distance (data not shown). Therefore, each BC carrying the information of a distinct group of GCs activates similarly the PC. Detecting the synchrony of multiple BCs may play an important role in integrating the spatial information over a wide range of GCs. As shown in Fig. 3.11, the dendritic inhibition works as a scaling factor for the excitatory inputs and shortens the membrane time constant to rapidly terminate membrane depolarization. Its broad frequency response property may suggest an important functional consequence of balancing the dendritic depolarization in order to prevent the activation of voltage-gated active conductances such as Ca^{2+} spikes (Llinas et al., 1968; London and Häusser, 2005; Miles et al., 1996).

In general, frequency tuning appears to be a major function for neuronal circuits, however, its property differs among preparations (Beierlein et al., 2003; Pouille and Scanziani, 2004; Mori et al., 2004; Lawrence and McBain, 2003). Depending on the type of information a circuit needs to process, the connectivity pattern of the neurons and the property of the synapses are different, which results in the various filtering properties. One concern which has not been taken into account in this study, is the ongoing activity of neurons and circuits *in vivo*, the so-called background activity. Background activity will change the membrane conductance of a neuron dynamically, or drive a synapse into its steady-state and cause oscillation in a circuit. It is of great interests to study whether circuit dynamics will be modified by the background activity and if so how. One way of this study is to conduct the measurement *in vivo* and an alternative way is to simulate the *in-vivo* like background activity in the brain slice through dynamic clamp or other stimulation methods.

4. DISCUSSION

References

- Abbott LF, Regehr WG (2004) Synaptic computation. *Nature* 431:796 – 803. 7, 14
- Abbott LF, Varela JA, Sen K, Nelson SB (1997) Synaptic Depression and Cortical Gain Control. *Science* 275:221–224. 14, 16
- Augustin I, Betz A, Herrmann C, Jo T, Brose N (1999) Differential expression of two novel munc13 proteins in rat brain. *Biochem. J.* 337:363–371. 54
- Augustin I, Korte S, Rickmann M, Kretzschmar HA, Sudhof TC, Herms JW, Brose N (2001) The Cerebellum-Specific Munc13 Isoform Munc13-3 Regulates Cerebellar Synaptic Transmission and Motor Learning in Mice. *J. Neurosci.* 21:10–17. 54
- Bao J, Reim K, Sakaba T (2010) Target-dependent feed-forward inhibition mediated by short-term synaptic plasticity in the cerebellum. *J. Neurosci.* (in press). 10
- Bao J (2007) Information content of synapses with realistic short-term dynamics. Master thesis. 31
- Barbour B (1993) Synaptic currents evoked in purkinje cells by stimulating individual granule cells. *Neuron* 11:759 – 769. 38, 40
- Basu J, Betz A, Brose N, Rosenmund C (2007) Munc13-1 C1 Domain Activation Lowers the Energy Barrier for Synaptic Vesicle Fusion. *J. Neurosci.* 27:1200–1210. 54, 66

REFERENCES

- Beierlein M, Fioravante D, Regehr WG (2007) Differential expression of posttetanic potentiation and retrograde signaling mediate target-dependent short-term synaptic plasticity. *Neuron* 54:949 – 959. 10, 38, 54, 61, 62
- Beierlein M, Gibson JR, Connors BW (2003) Two Dynamically Distinct Inhibitory Networks in Layer 4 of the Neocortex. *J Neurophysiol* 90:2987–3000. 41, 67, 68, 69
- Blitz DM, Regehr WG (2005) Timing and specificity of feed-forward inhibition within the lgn. *Neuron* 45:917 – 928. 60
- Borst JGG, Sakmann B (1996) Calcium influx and transmitter release in a fast cns synapse. *Nature* 383:431 – 434. 4
- Borst JGG, Sakmann B (1998) Facilitation of presynaptic calcium currents in the rat brainstem. *J Physiol.* 15:149 –155. 15
- Boyd IA, Martin AR (1956) The end-plate potential in mammalian muscle. *The Journal of Physiology* 132:74–91. 5
- Brown TH, Kairiss EW, Keenan CL (1990) Hebbian synapses: Biophysical mechanisms and algorithms. *Annual Review of Neuroscience* 13:475–511. 6
- Caillard O, Moreno H, Schwaller B, Llano I, Celio MR, Marty A (2000) Role of the calcium-binding protein parvalbumin in short-term synaptic plasticity. *Proceedings of the National Academy of Sciences of the United States of America* 97:13372–13377. 36
- Callaway EM (2004) Feedforward, feedback and inhibitory connections in primate visual cortex. *Neural Networks* 17:625 – 632. 60
- Chadderton P, Margrie TW, Häusser M (2004) Integration of quanta in cerebellar granule cells during sensory processing. *Nature* 428:856–860. 46, 68
- Chance FS, Nelson SB, Abbott LF (1998) Synaptic Depression and the Temporal Response Characteristics of V1 Cells. *J. Neurosci.* 18:4785–4799. 14

REFERENCES

- Cryan JF, Holmes A (2005) The ascent of mouse: advances in modelling human depression and anxiety. *Nature Reviews Drug Discovery* 4:775–790. 22
- D’Angelo E, Zeeuw CID (2009) Timing and plasticity in the cerebellum: focus on the granular layer. *Trends in Neurosciences* 32:30 – 40. 60
- Davies CH, Davies SN, Collingridge GL (1990) Paired-pulse depression of monosynaptic GABA-mediated inhibitory postsynaptic responses in rat hippocampus. *The Journal of Physiology* 424:513–531. 10
- Delaney K, Zucker R, Tank D (1989) Calcium in motor nerve terminals associated with posttetanic potentiation. *J. Neurosci.* 9:3558–3567. 9
- Diana MA, Levenes C, Mackie K, Marty A (2002) Short-Term Retrograde Inhibition of GABAergic Synaptic Currents in Rat Purkinje Cells Is Mediated by Endogenous Cannabinoids. *J. Neurosci.* 22:200–208. 61
- Dittman JS, Kreitzer AC, Regehr WG (2000) Interplay between Facilitation, Depression, and Residual Calcium at Three Presynaptic Terminals. *J. Neurosci.* 20:1374–1385. 8, 11, 14, 31, 40, 61
- Dittman JS, Regehr WG (1998) Calcium Dependence and Recovery Kinetics of Presynaptic Depression at the Climbing Fiber to Purkinje Cell Synapse. *J. Neurosci.* 18:6147–6162. 15
- Eccles JC, Llinas R, Sasaki K (1966a) Parallel Fibre Stimulation and the Responses Induced thereby in the Purkinje Cells of the Cerebellum. *Experimental Brain Research* 1:17–39. 35
- Eccles JC, Llinas R, Sasaki K (1966b) The excitatory synaptic action of climbing fibres on the Purkinje cells of the cerebellum. *J Physiol* 182:268–296. 68
- Eccles JC, Llinas R, Sasaki K (1966c) The Inhibitory Interneurons within the Cerebellar Cortex. *Experimental Brain Research* 1:1–16. 68
- Feng TP (1941) The change in the end-plate potential during and after prolonged stimulation. *Chin.J.Physiol.* 13:79–107. 7

REFERENCES

- Foffani G, Morales-Botello ML, Aguilar J (2009) Spike Timing, Spike Count, and Temporal Information for the Discrimination of Tactile Stimuli in the Rat Ventrobasal Complex. *J. Neurosci.* 29:5964–5973. 15
- Fortune ES, Rose GJ (2002) Roles for short-term synaptic plasticity in behavior. *Journal of Physiology-Paris* 96:539–545. 14
- Fuhrmann G, Segev I, Markram H, Tsodyks M (2002) Coding of Temporal Information by Activity-Dependent Synapses. *J Neurophysiol* 87:140–148. 14, 16
- Goldman MS, Maldonado P, Abbott LF (2002) Redundancy Reduction and Sustained Firing with Stochastic Depressing Synapses. *J. Neurosci.* 22:584–591. 14
- Häusser M, Clark BA (1997) Tonic synaptic inhibition modulates neuronal output pattern and spatiotemporal synaptic integration. *Neuron* 19:665 – 678. 68
- Hefft S, Jonas P (2005) Asynchronous gaba release generates long-lasting inhibition at a hippocampal interneuron-principal neuron synapse. *Nat Neurosci* 8:1319–1328. 41, 67
- Isaacson JS, Solis JM, Nicoll RA (1993) Local and diffuse synaptic actions of gaba in the hippocampus. *Neuron* 10:165 – 175. 10
- Isope P, Barbour B (2002) Properties of Unitary Granule Cellright-arrowPurkinje Cell Synapses in Adult Rat Cerebellar Slices. *J. Neurosci.* 22:9668–9678. 40, 61, 67
- Jones MV, Westbrook GL (1996) The impact of receptor desensitization on fast synaptic transmission. *Trends in Neurosciences* 19:96 – 101. 9, 62
- Jorntell H, Ekerot CF (2006) Properties of Somatosensory Synaptic Integration in Cerebellar Granule Cells In Vivo. *J. Neurosci.* 26:11786–11797. 46, 68
- Katz B (1969) *The Release of Neural Transmitter Substances*. Liverpool University Press, Liverpool, United Kingdom. 5, 9, 31

REFERENCES

- Katz P, Kirk M, Govind C (1993) Facilitation and depression at different branches of the same motor axon: evidence for presynaptic differences in release. *J. Neurosci.* 13:3075–3089. 61
- Klyachko V, Stevens C (2006) Excitatory and feed-forward inhibitory hippocampal synapses work synergistically as an adaptive filter of natural spike trains. *PLoS Biology* 4:1187 – 1200. 68
- Koch C (1999) *Biophysics of Computation* Oxford University Press. 2, 33
- Konnerth A, Llano I, Armstrong CM (1990) Synaptic currents in cerebellar Purkinje cells. *Proceedings of the National Academy of Sciences of the United States of America* 87:2662–2665. 61
- Kosaka T, Kosaka K, Nakayama T, Hunziker W, Heizmann CW (1993) Axons and axon terminals of cerebellar Purkinje cells and basket cells have higher levels of parvalbumin immunoreactivity than somata and dendrites: quantitative analysis by immunogold labeling. *Experimental Brain Research* 93:483–491. 36
- Kreitzer AC, Regehr WG (2000) Modulation of Transmission during Trains at a Cerebellar Synapse. *J. Neurosci.* 20:1348–1357. 9, 54
- Lawrence JJ, McBain CJ (2003) Interneuron diversity series: Containing the detonation - feedforward inhibition in the ca3 hippocampus. *Trends in Neurosciences* 26:631 – 640. 54, 61, 62, 69
- Liley AW, North KAK (1953) An electrical investigation of effects of repetitive stimulation on mammalian neuromuscular junction. *J. Neurophysiol.* 16:509–527. 10, 12
- Lisman JE (1997) Bursts as a unit of neural information: making unreliable synapses reliable. *Trends in Neurosciences* 20:38 – 43. 14
- Llinas R, Nicholson C, Freeman JA, Hillman DE (1968) Dendritic Spikes and Their Inhibition in Alligator Purkinje Cells. *Science* 160:1132–1135. 69
- London M, Häusser M (2005) Dendritic computation. *Annual Review of Neuroscience* 28:503–532. 69

REFERENCES

- Maass W, Markram H (2002) Synapses as dynamic memory buffers. *Neural Networks* 15:155 – 161. 14
- Marcaggi P, Attwell D (2005) Endocannabinoid signaling depends on the spatial pattern of synapse activation. *Nature Neuroscience* 8:776 – 781. 38
- Markram H, Pikus D, Gupta A, Tsodyks M (1998) Potential for multiple mechanisms, phenomena and algorithms for synaptic plasticity at single synapses. *Neuropharmacology* 37:489 – 500. 14
- Markram H, Toledo-Rodriguez M, Wang Y, Gupta A, Silberberg G, Wu C (2004) Interneurons of the neocortical inhibitory system. *Nature Reviews Neuroscience* 5:793–807. 37
- Markram H, Wang Y, Tsodyks M (1998) Differential signaling via the same axon of neocortical pyramidal neurons. *PNAS* 95:5323–5328. 12, 31
- Miles R, Tth K, Gulys AI, Hjos N, Freund TF (1996) Differences between somatic and dendritic inhibition in the hippocampus. *Neuron* 16:815 – 823. 67, 69
- Millar AG, Zucker RS, Ellis-Davies GCR, Charlton MP, Atwood HL (2005) Calcium Sensitivity of Neurotransmitter Release Differs at Phasic and Tonic Synapses. *J. Neurosci.* 25:3113–3125. 4
- Mintz IM, Sabatini BL, Regehr WG (1995) Calcium control of transmitter release at a cerebellar synapse. *Neuron* 15:675 – 688. 4
- Mittmann W, Koch U, Häusser M (2005) Feed-forward inhibition shapes the spike output of cerebellar Purkinje cells. *J Physiol* 563:369–378. 38
- Moore E, Shannon C (1956) Reliable circuits using less reliable relays. *J. Franklin Inst.* 262:191–208. 5
- Mori M, Abegg M, Ghwiler B, Gerber U (2004) A frequency-dependent switch from inhibition to excitation in a hippocampal unitary circuit. *nature* 431:453–456. 68, 69

REFERENCES

- Neher E, Sakaba T (2008) Multiple roles of calcium ions in the regulation of neurotransmitter release. *Neuron* 59:861 – 872. 4
- Niven JE, Laughlin SB (2008) Energy limitation as a selective pressure on the evolution of sensory systems. *J Exp Biol* 211:1792–1804. 68
- Palay SL, Chan-Palay V (1974) *Cerebellar Cortex: Cytology and Organization* Springer-Verlag, Berlin. 35, 41, 67, 69
- Pan B, Zucker RS (2009) A general model of synaptic transmission and short-term plasticity. *Neuron* 62:539 – 554. 4
- Patlak JB, Ortiz M (1986) Two modes of gating during late Na⁺ channel currents in frog sartorius muscle. *The Journal of General Physiology* 87:305–326. 5
- Pouille F, Scanziani M (2004) Routing of spike series by dynamic circuits in the hippocampus. *nature* 429:717–723. 67, 68, 69
- Prinz AA, Abbott LF, Marder E (2004) The dynamic clamp comes of age. *Trends in Neurosciences* 27:218 – 224. 28, 56
- Purves D, Augustine GJ, Fitzpatrick D, Katz LC, LaMantia AS, McNamara JO, Williams SM (2001) *Neuroscience* Sinauer Associates Inc.,U.S. 20
- Regehr W, Delaney K, Tank D (1994) The role of presynaptic calcium in short-term enhancement at the hippocampal mossy fiber synapse. *J. Neurosci.* 14:523–537. 9
- Reyes A, Lujan R, Rozov A, Burnashev N, Somogyi P, Sakmann B (1998) Target-cell-specific facilitation and depression in neocortical circuits. *Nat. Neurosci.* 1:279–285. 54, 61, 62
- Rosenmund C, Clements J, Westbrook G (1993) Nonuniform probability of glutamate release at a hippocampal synapse. *Science* 262:754–757. 61
- Rosenmund C, Sigler A, Augustin I, Reim K, Brose N, Rhee JS (2002) Differential control of vesicle priming and short-term plasticity by munc13 isoforms. *Neuron* 33:411–424. 66

REFERENCES

- Sakaba T (2008) Two Ca^{2+} -dependent steps controlling synaptic vesicle fusion and replenishment at the cerebellar basketcell terminal. *Neuron* 57:406 – 419. 41, 68
- Scanziani M, Ghwiler BH, Charpak S (1998) Target cell-specific modulation of transmitter release at terminals from a single axon. *Proceedings of the National Academy of Sciences of the United States of America* 95:12004–12009. 61
- Schneggenburger R, Neher E (2000) Intracellular calcium dependence of transmitter release rates at a fast central synapse. *Nature* 406:889–893. 4
- Silberberg G, Wu C, Markram H (2004) Synaptic dynamics control the timing of neuronal excitation in the activated neocortical microcircuit. *The Journal of Physiology* 556:19–27. 14
- Sims RE, Hartell NA (2005) Differences in Transmission Properties and Susceptibility to Long-Term Depression Reveal Functional Specialization of Ascending Axon and Parallel Fiber Synapses to Purkinje Cells. *J. Neurosci.* 25:3246–3257. 62
- Sims RE, Hartell NA (2006) Differential Susceptibility to Synaptic Plasticity Reveals a Functional Specialization of Ascending Axon and Parallel Fiber Synapses to Cerebellar Purkinje Cells. *J. Neurosci.* 26:5153–5159. 61
- Somogyi P, Klausberger T (2005) Defined types of cortical interneurone structure space and spike timing in the hippocampus. *J Physiol* 562:9–26. 37
- Stell BM, Rostaing P, Triller A, Marty A (2007) Activation of Presynaptic GABAA Receptors Induces Glutamate Release from Parallel Fiber Synapses. *J. Neurosci.* 27:9022–9031. 61
- Stevens CF, Wesseling JF (1998) Activity-Dependent Modulation of the Rate at which Synaptic Vesicles Become Available to Undergo Exocytosis. *Neuron* 21:415–424. 15
- Sultan F, Bower JM (1998) Quantitative Golgi study of the rat cerebellar molecular layer interneurons using principal component analysis. *The Journal of Comparative Neurology* 393:353–373. 36, 67

REFERENCES

- Swadlow HA (2003) Fast-spike Interneurons and Feedforward Inhibition in Awake Sensory Neocortex. *Cereb. Cortex* 13:25–32. 60
- Thorpe S, Delorme A, Rullen RV (2001) Spike-based strategies for rapid processing. *Neural Networks* 14:715 – 725. 15
- Tong G, Jahr CE (1994) Multivesicular release from excitatory synapses of cultured hippocampal neurons. *Neuron* 12:51 – 59. 9, 62, 64, 66
- Trussell LO, Fischbach GD (1989) Glutamate receptor desensitization and its role in synaptic transmission. *Neuron* 3:209 – 218. 9, 62, 63
- Tsodyks MV, Markram H (1997) The neural code between neocortical pyramidal neurons depends on neurotransmitter release probability. *PNAS* 94:719–723. 10, 12, 14, 31, 56, 57
- Varela JA, Sen K, Gibson J, Fost J, Abbott LF, Nelson SB (1997) A Quantitative Description of Short-Term Plasticity at Excitatory Synapses in Layer 2/3 of Rat Primary Visual Cortex. *J. Neurosci.* 17:7926–7940. 9, 10, 12, 31
- Vincent P, Marty A (1993) Neighboring cerebellar purkinje cells communicate via retrograde inhibition of common presynaptic interneurons. *Neuron* 11:885 – 893. 68
- Vincent P, Marty A (1996) Fluctuations of inhibitory postsynaptic currents in Purkinje cells from rat cerebellar slices. *J Physiol* 494:183–199. 36, 67
- Wang LY, Kaczmarek LK (1998) High-frequency firing helps replenish the readily releasable pool of synaptic vesicles. *Nature* 394:384–388. 15
- Wright SN, Brodwick MS, Bittner GD (1996) Calcium currents, transmitter release and facilitation of release at voltage-clamped crayfish nerve terminals. *The Journal of Physiology* 496:363–378. 54
- Wu LG, Saggau P (1997) Presynaptic inhibition of elicited neurotransmitter release. *Trends in Neurosciences* 20:204 – 212. 10

REFERENCES

Yuste R, Konnerth A (2005) *Imaging in Neuroscience and Development: a Laboratory Manual* Cold Spring Harbor Press. 9

Zilberter Y, Kaiser KM, Sakmann B (1999) Dendritic gaba release depresses excitatory transmission between layer 2/3 pyramidal and bitufted neurons in rat neocortex. *Neuron* 24:979 – 988. 10

Zucker RS (1989) Short-term synaptic plasticity. *Annual Review of Neuroscience* 12:13–31. 9

Zucker RS, Regehr WG (2002) Short-term synaptic plasticity. *Annu. Rev. Physiol.* 64:355–405. 7, 39

Zucker RS (1973) Changes in the statistics of transmitter release during facilitation. *The Journal of Physiology* 229:787–810. 15

Declaration

I hereby declare that I have produced this thesis independently without the prohibited assistance of third parties and without making use of aids other than those specified; notions taken over directly or indirectly from other sources have been identified as such. This paper has not previously been presented in identical or similar form to any other German or foreign examination board.

The thesis work was conducted from 2007 to 2010 under the supervision of Dr. Takeshi Sakaba at Max-Planck Institute for Biophysical Chemistry.

Göttingen, 07. June. 2010

Curriculum Vitae

Jin Bao

Gender: Female

Date of birth: 30, Oct 1979

Place of birth: Hefei, China

Nationality: China

EDUCATION

09/1997-07/2002	Undergraduate study on BioMedical Engineering, Zhejiang University, China
07/2002	Bachelor's degree of Engineering
09/2002-07/2005	Graduate study on Physics, Tsinghua University, China
09/2005-03/2007	MSc. Student of International Max-Planck Research School Neuroscience program, University of Göttingen, Germany
10/2007	Master degree of Neuroscience
Since 04/2007	PhD student of Max-Planck Institute for Biophysical Chemistry and Göttingen University, Germany

PUBLICATIONS

Huang, CH, **Bao, J.**, and Sakaba, T. Multivesicular Release Differentiates the Reliability of Synaptic Transmission between the Visual Cortex and the Somatosensory Cortex. *J. Neurosci.*, 30: 11994 - 12004 (2010).

Bao, J., Reim, K., Sakaba, T. Target-dependent feed-forward inhibition mediated by short-term synaptic plasticity in the cerebellum. *J.*

Neurosci., 30:8171-8179 (2010).

Wang, Y., **Bao, J.**, Sheng, X., Li, P., Ma, H. Probing Type I/III Collagen in Dennis using Second Harmonic Generation Imaging. ACTA LASER BIOLOGY SINICA 14(4):274-278 (2005)